SMART-Editor: A Multi-Agent Framework for Human-Like Design Editing with Structural Integrity

Anonymous ARR submission

Abstract

We present **SMART-Editor**, a framework for compositional layout and content editing across structured (posters, websites) and unstructured (natural images) domains. Unlike prior models that perform local edits, **SMART-Editor** preserves global coherence through two strategies: Reward-Refine, an inference-time reward-guided refinement method, and RewardDPO, a training-time preference optimization approach using reward-aligned layout pairs. To evaluate model performance, we introduce **SMARTEdit-Bench**, a benchmark covering multi-domain, cascading edit scenarios. **SMART-Editor** outperforms strong baselines like InstructPix2Pix and HIVE, with RewardDPOachieving up to 15% gains in structured settings and Reward-Refine showing advantages on natural images. Automatic and human evaluations confirm the value of reward-guided planning in producing semantically consistent and visually aligned edits.

1 Introduction

Layout and scene editing is a cornerstone of multimodal reasoning, encompassing tasks such as poster restructuring, webpage reflow, and natural image transformation (Suri et al., 2024; Zhu et al., 2024; Gani et al., 2024; Tanaka et al., 2024; Lin et al., 2024). These edits often go beyond simple object manipulations and require coordinated adjustments across spatial, semantic, and stylistic dimensions (Jia et al., 2024; Feng et al., 2023a; Lin et al., 2023). Instructions like "Insert a video section at the middle" (Figure 1) require cascading edits such as identifying an insertion point in layout hierarchy, shifting subsequent sections to preserve flow, aligning with adjacent regions, and updating labels and narrative rhythm for coherence.

When *humans* learn how to draw or typset, they learn about the basics of composition and balance (Golomb, 1987), but it remains unclear whether large language models (LLMs) or visual LMs

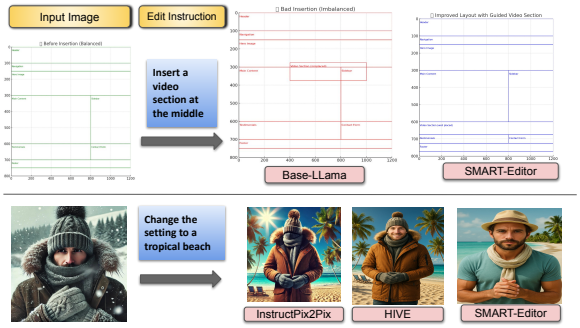

Figure 1: Unlike InstructPix2Pix (Brooks et al., 2023), HIVE (Zhang et al., 2024b), and Base-LLama, which apply edits locally and often fail to maintain coherence, **SMART-Editor** performs structured layout edits and visual transformations with compositional reasoning—anticipating cascading effects and preserving global alignment and semantic consistency.

(VLMs) can propagate edits in a structured and semantically coherent manner. These tasks are critical for scientific communication (Lozano, 2014), where even a single misplaced section or inconsistent scene can undermine clarity, or usability.

To explore this challenge, we introduce the notion of a **SMART-EDIT**—an edit that (a) adheres semantically to the instruction, (b) minimizes disruption to unrelated content, (c) preserves spatial coherence and alignment, and (d) anticipates and resolves cascading effects (formalized in Section 2). We further present **SMARTEdit-Bench** (Section 3), a benchmark designed to evaluate compositional edit reasoning in LLMs and VLMs across three domains: scientific posters, web layouts, and natural images. Each instance in the benchmark features a real-world or curated edit sourced from datasets such as SciPostLayout (Tanaka et al., 2024), Design2Code (Si et al., 2025), and HQEdit (Hui et al., 2024), comprising an initial scene, a human-verified SMART-EDIT instruction, and a target layout/image requiring multi-step semantic and structural updates. Unlike prior datasets focused on isolated edits (Table 1), **SMARTEdit-**

Dataset / System	Domain(s)	Edit-Aware	Comp. Reasoning	Cascading	Instruction	Eval Scope	Notable Features
InstructEdit (Wang et al., 2023)	Natural Images	✓	–	–	Natural Language	Visual, Mask Accuracy	LLM + segmentation + SD for multi-object edits.
PostScoreEdit	Social Media	✓	–	–	Prompt Paraphrasing	Engagement, Human Ratings	Paraphrase+rank to boost audience engagement.
FFCLIP (Radford et al., 2021)	Faces, Cars, Churches	✓	Partial	–	Free-form Text	CLIP Alignment	StyleGAN latent editing via CLIP alignment.
DocEdit-v2 (Suri et al., 2024)	Structured Docs	✓	Local	–	Free/Structured	DOM Tree, CSS IoU	LMM-based HTML editing + reformulation.
LayoutGPT (Feng et al., 2023b)	2D/3D Layouts	–	✓	–	Prompt Only	Layout Plausibility	CSS-like layout synthesis with spatial reasoning.
COLE (Jia et al., 2024)	Graphic Design	–	Hierarchical	–	Design Intent	Visual + Typographic	JSON + image gen for typography and layout.
SciPostLayout (Tanaka et al., 2024)	Scientific Posters	–	–	–	Layout Only	Visual Structure	Poster layout generation only, no edit modeling.
LayoutCoT (Shi et al., 2025)	Posters, UI Layouts	–	CoT Only	–	CoT Prompting	Visual Coherence	Prompt-based spatial reasoning, no edit ops.
SMARTEdit-Bench (Ours)	Posters, Web, Images	✓	✓	✓	Implicit instructions requiring Cascaded-Reasoning	Visual, Semantic, Structural	Multi-domain, layout propagation, semantic + visual edit cascades.

Table 1: Comparison of SMARTEdit-Bench with prior datasets. Our benchmark uniquely supports multi-domain, instruction-grounded cascading edits with compositional reasoning. Related works are described in Appendix 10.

Bench is designed to evaluate the ability of models to perform globally coherent, multi-step edits to maintain *human-like design integrity*.

We observe that base LLMs/VLMs like LLaMA, Qwen, LLaVA, GPT4-o and Gemini-pro can follow instructions superficially (edit adherence $>=$ 4.0), but fail to preserve deeper layout reasoning: narrative coherence drops by over 15% during section reordering, and layout alignment degrades sharply during insert/delete operations (Table 2, 3, 4). Cross-sectional consistency is especially fragile when instructions induce global changes (e.g., regrouping content or propagating section deletions). To address these limitations, we introduce **SMART-Editor**, a modular agentic framework that coordinates planning, execution, critique, and optimization (Section 4 and Figure 2). The **Action Agent** translates edit instructions into layout operations, which are applied by the **Executor**. A **Critique Agent** then evaluates the output across structured reward axes (e.g., overlap, whitespace, coherence) and produces actionable feedback in natural language. This feedback/new action plan guides the **Optimizer Agent**, which operates in two modes: (1) **Reward-Refine**, which uses critiques to revise the initial plan in an iterative loop until all quality checks are satisfied; and (2) **RewardDPO**, which fine-tunes the model using preference pairs filtered by reward alignment to generalize better layout reasoning policies. Across posters, webpages, and natural images, SMART-Editor improves layout alignment (+0.3–0.5), narrative and cross-sectional consistency (up to +0.2), and visual plausibility (Figure 3, 4).

2 Evaluation of 'SMARTness' of an Edit?

Inspired by the evaluation metrics used by prior layout generation works (Tanaka et al., 2024; Lin et al., 2023; Hui et al., 2024; Zhang et al., 2024b), we formalize the notion of **SMART-Edit** as an edit operation that, when applied to structured or unstructured visual content, satisfies a set of post-edit quality constraints in structured domain ((Definitions and Mathematical Formulations in Appendix 12.1) such as **1) Edit Adherence** verifies whether the edit instruction is faithfully executed **2) Narrative Coherence** ensures logical section ordering (e.g., *Methods* before *Results*) is preserved. Violations are detected by prompting GPT-4o on expected order pairs **3) Cross-Sectional Consistency** evaluates whether semantically linked elements (e.g., captions and figures, objects and context) remain aligned. Contradictions are flagged via entailment-based GPT-4o prompts **4) Visual-Spatial Layout** captures design quality through three components: overlap penalty (discouraging collisions), whitespace penalty (encouraging compactness), and alignment reward (favoring grid-aligned layouts). However, in unstructured natural images , we formulate four core capabilities (Definitions and Mathematical Formulations in Appendix 12.3) **1) Edit Adherence (EA)** - Same as before, **2) Semantic match (SM)** : Compute the CLIP similarity between the textual instruction and the generated image, **3) Object Size and Realism (Overlap)** : Check if the edited image contains objects that appear too large, too small, or overlap unnaturally, **4) Depth Layering and Occlusion (DL)** Evaluates if the spatial layering of objects appear real and not floating.

3 SMARTEdit-Bench

Existing datasets (Table 1) largely focus on local, explicit edits, and fail to capture the implicit, compositional nature of real-world editing—where a single instruction often triggers global layout or scene changes. To address this, we introduce **SMARTEdit-Bench**, a multi-domain benchmark covering structured (posters, webpages) and unstructured (natural images) inputs. Each example includes a natural language instruction, a human-edited output, and metadata annotated with edit type (A manual analysis of 200 real-world edit examples identifies five types of structural edits: Reordering, Insertion, Object Replacement, Content Grouping, and Deletion (Table 9)—which are implicit in nature (without specifying how to edit)

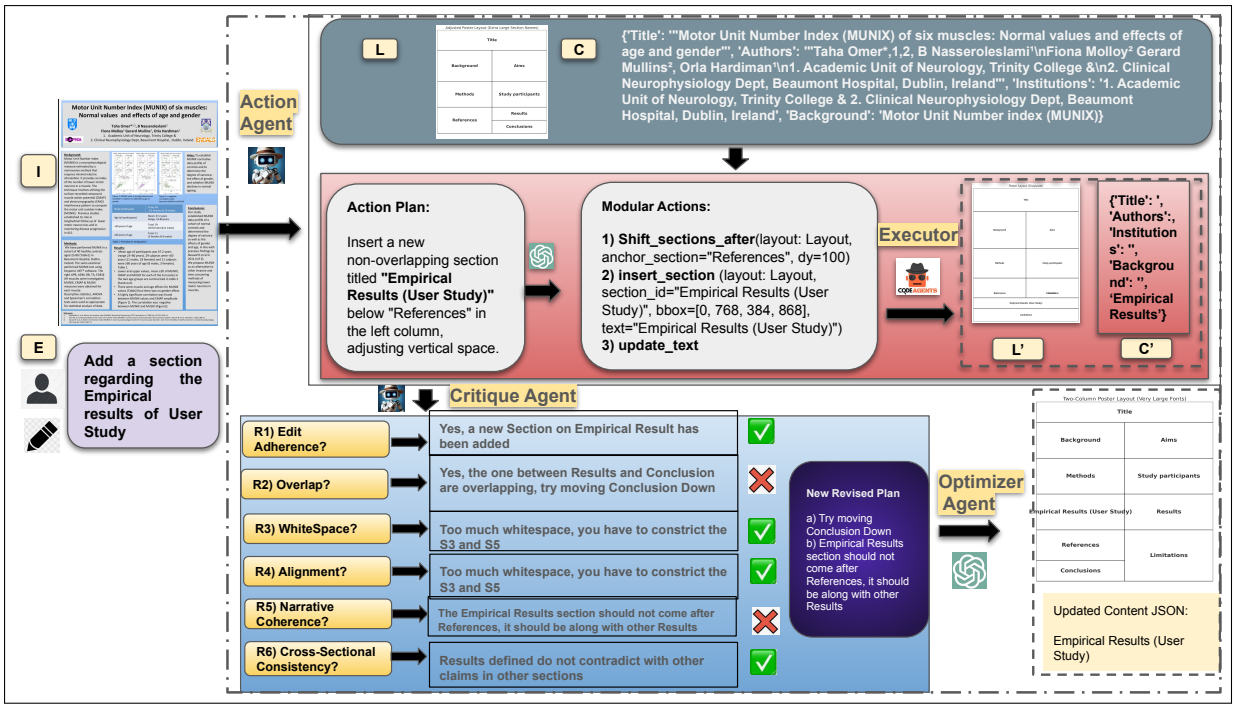

Figure 2: Overview of **SMART-Editor** (Reward-Refine) on structured image (Poster). Given a poster image, and a high-level edit instruction, SMART-Editor generates an action plan and applies geometric edits (**Action Agent**). The first-draft output is evaluated on several aspect (**Critique Agent**). Any violations trigger natural language feedback used to revise layout and content in an iterative loop, enabling reward-guided editing (**Optimizer Agent**).

and necessitate cascading, multi-region updates). Dataset statistics are shown in Table 8.[1]

SMARTEdit-Bench – Webpages. We divide the dataset into two parts: (a) Real-World Edits: We extract layout-altering commits from github.io repositories by comparing HTML snapshots before and after structural changes. Stylistic edits are removed using two signals: low DOM tree edit distance and high semantic similarity, indicating minimal structural change. GPT-4V generates natural language instructions by comparing before/after screenshots. This results in 564 triplets (Before Commit, Edit Instruction, After Commit), each manually reviewed and refined by the first author to ensure they are '*Smart-Edits*'. (b) Synthetic Edits: Layouts are sampled from the Design2Code dataset(Si et al., 2025). GPT-4o generates implicit, high-level edit instructions. An expert annotator ensures the instruction leads to compositional layout updates; otherwise, both instruction and layout are revised manually. This yields 510 high-quality synthetic triplets.

SMARTEdit-Bench – Posters. We generate 1,200 synthetic poster edits using SciPostLayout (Tanaka et al., 2024), prompting GPT-4V/4o to propose compositional layout transformations. All outputs are manually reviewed to remove trivial or overly explicit edits. Two expert annotators label 250 human-edited posters with edit types and reasoning dimensions, forming a gold test set. An additional 2,000 synthetic edits support training and preference modeling.

SMARTEdit-Bench – Natural Images. To cover unstructured visual edits, we adopt examples from the HQ-Edit (Hui et al., 2024) dataset. Each instance contains an image, an instruction, and an edited output with aligned bounding boxes. We manually filter out 500 edits which require spatial reasoning and cascaded changes, and use the gold outputs for evaluation.

4 SMART-Editor

We formulate *SMART-Editing* as a structure-aware generation task guided by natural language instructions. To this end, we propose the **SMART-Editor** pipeline, which orchestrates a trilateral collaboration among three core agents—**Action**, **Critique**, and **Optimizer**—to perform semantically faithful and visually coherent layout-content editing grounded in an input image and edit instruction. The system takes as input a raw image I and an edit instruction E, from which it generates an edited

[1]We plan to release the dataset upon acceptance and this is intended only for research purposes. All source datasets are publicly available under CC-BY and MIT License.

image I' following the edit instruction.

1. Action Agent. First, the **Action Agent** takes a raw input image I and edit instruction E, and outputs a first-pass edited layout-content pair (L', C'). It first parses I into an initial layout $L = \{(o_i, \mathbf{b}_i)\}_{i=1}^{N}$, where o_i denotes a visual region (e.g., section type or object label), $\mathbf{b}_i = (x_i, y_i, x_i', y_i') \in \mathbb{R}^4$ is its bounding box. In parallel, it extracts associated textual content C to these regions (Details in Appendix 11.1).

After pre-processing, given the parsed input of layout-content pair (L, C) and instruction E, an action plan is first generated using LLM (Action-Plan in Figure 2) followed by generating a symbolic edit plan $A = [a_1, a_2, \ldots, a_k] = \texttt{LLM_Plan}(E, L, C)$, where each action a_j corresponds to a structured operation from the Action Registry (such as translate, reorder etc.) which are present in Table 10 (Refer to Modular Actions in Figure 2). The executor agent then executes each of the modular actions in A to yield the first draft of the edited output (L', C'), which serves as input to next stage. Refer to Appendix 11.3 for details.

Critique Agent. The **Critique Agent** evaluates the semantic and visual quality of the edited layout-content pair (L', C'), generating both a scalar reward score $R(L', C')$ and structured, actionable feedback for refinement (see Appendix 11.4). As detailed in Section 2, the criteria for assessing edits differ across structured and unstructured domains. For *structured domains*, we employ a combination of heuristic checks and LLM-based prompting (Appendix 12.1) to compute reward components aligned with the axes R1–R6 in Figure 2, enabling diagnosis of specific issues and suggestions for improvement (e.g., the Overlap Critic might note, "*Yes, the one between Results and Conclusion are overlapping, try moving Conclusion down*"). For *unstructured images*, the agent evaluates four core dimensions—Edit Adherence, Semantic Consistency, Depth and Occlusion, and Size Realism—as defined in Section 2 and further detailed in Appendix 11.4, providing targeted feedback to guide coherent visual refinement.

Optimizer Agent. We compute the composite reward as a weighted sum of interpretable components: $R(L', C') = \sum_{k=1}^{K} \lambda_k \cdot r_k(L')$, where each r_k captures a specific quality axis and $\lambda_k \in \mathbb{R}$ is a tunable weight (k=1 in our case). If $R(L', C')$ falls below a threshold, the **Optimizer** agent explores two complementary strategies for optimizing generation under reward-defined constraints: an inference-time refinement loop-based method (Reward-Refine) and a training-time preference distillation approach (RewardDPO).

1) Iterative Refinement (Reward-Refine). This method performs reward-guided self-correction through iterative inference (Algorithm 1). At iteration $t = 1$, beam search is used to sample k candidate layout-content pairs $(L_i^{(t)}, C_i^{(t)})$ conditioned on the previous state $(L^{(t-1)}, C^{(t-1)})$ and the instruction E. Based on the critique feedback, we convert the suggested improvement into a revised plan expressed in the structured *action space* defined by the *Action Registry* (Section 10). These symbolic actions guide the generation of new candidate layouts, and beam search is again employed to sample alternatives and select the best one by computing the reward for each. The best candidate under the reward function is selected as $(L^{(t)}, C^{(t)}) = \arg\max_{(L,C)} R(L)$. This process continues iteratively until all constraints are satisfied or a maximum number of refinement steps is reached. The final output is the converged layout-content pair $(L^*, C^*) = (L^{(T)}, C^{(T)})$, emulating a human-in-the-loop editor through critique-to-action planning.

2) Reward-Aligned Preference Optimization (RewardDPO) To address runtime and initialization limitations of inference-time refinement, we propose **RewardDPO**, a training-time framework that distills reward-aligned preferences into the model via contrastive supervision over structured perturbations (Algorithm 2). This actually takes the initial output L_0 after preprocessing in the **Action Agent** as input, uses **Critique Agents** to generate preference data, and finally generates optimized layout L^* as output (We skip optimizing the content using DPO, as it improves well in 1 single iteration in **Reward-Refine**). It follows 3 steps as described below:

Supervised Finetuning. We begin with a supervised finetuning (SFT) stage, where the model f_θ is trained on triplets $(L_0^{(i)}, E^{(i)}, L_{\text{target}}^{(i)}) \in \mathcal{D}_{\text{SFT}}$. The model is optimized using a log-likelihood objective: $\mathcal{L}_{\text{SFT}}(\theta) = -\sum_{i=1}^{N} \log P_\theta(L_{\text{target}}^{(i)} \mid E^{(i)}, L_0^{(i)})$.

Preference Pair Generation via Reward-Aligned Contrastive Supervision. Supervised fine-tuning typically exposes models to a single

"ideal" layout per instruction, limiting their ability to reason about the relative quality of edits. To address this, we construct contrastive preference pairs (L^+, L^-), where L^+ is verifiably better than L^- based on a composite reward function: $R(L) = \sum_{k=1}^{K} \lambda_k \cdot r_k(L)$, which aggregates multiple quality dimensions such as layout alignment, narrative flow, and visual plausibility.

For positive examples L^+, we primarily use gold-standard human-edited layouts when available (e.g., in SMARTEditBench). In cases where human edits are unavailable, we sample multiple candidate layouts from a base model and select the one with the highest reward score, while filtering out invalid candidates (e.g., layouts with overlapping elements, missing sections, or visual artifacts).

Negative examples L^- are created by applying targeted degradations to L^+ using transformation functions $T_k \in \mathcal{T}$, which are designed to introduce specific types of errors. In structured domains, these include misplacing sections (e.g., placing "Results" above "Methods"), inducing overlaps, misaligning bounding boxes, or distorting whitespace. In unstructured domains, we introduce implausible edits such as unrealistic object size, semantic mismatches (e.g., "cat on the sky"), or incorrect depth layering. We retain a pair only if the degradation results in a reward difference of at least δ, i.e., $R(L^+) - R(L^-) \geq \delta$, and the negative example violates at least one hard constraint (e.g., HASOVERLAP is true or BREAKSSEMANTICORDER is true). The final preference dataset is defined as $\mathcal{D}_{\text{pref}} = \{(I, L_0, L^+, L^-) \mid \Delta R \geq \delta \text{ and } L^- \text{ violates constraint}\}$, enabling supervision-free contrastive learning that trains the model not only to follow layout instructions but also to internalize design principles such as clarity, structure, and coherence.

Direct Preference Optimization. Given preference pairs (I, L_0, L^+, L^-), we train the model using the Direct Preference Optimization (DPO) (Rafailov et al., 2024) objective, defined as $\mathcal{L}_{\text{DPO}}(\theta) = -\log \frac{e^{\beta \log P_\theta(L^+|I,L_0)}}{e^{\beta \log P_\theta(L^+|I,L_0)} + e^{\beta \log P_\theta(L^-|I,L_0)}}$, where β controls the sharpness of the preference signal. Unlike SFT, DPO explicitly aligns generation with structural and semantic layout quality, enabling the model to prefer globally coherent outputs in a single forward pass.

At inference time, the **RewardDPO** model directly generates a high-quality layout $L^* = f_\theta(L_0, E)$ in a single forward pass, without requiring iterative refinement.

Model	Set.	EA ↑	Narr. ↑	XSec ↑	Ovlp ↓	WSpc ↓	Algn ↑
LPrompter		4.29	0.44	0.62	84	4.9	33.4
GPT-4o	ZS	4.52	0.43	0.61	58	3.5	35.0
	FS	4.60	0.44	0.63	60	3.6	35.5
	CoT	4.65	0.46	0.65	55	3.4	36.0
	SE	**4.70**	0.47	**0.67**	52	3.2	36.5
Gemini-Pro	ZS	4.48	0.41	0.60	60	3.8	34.5
	FS	4.55	0.45	0.62	62	3.9	35.0
	CoT	4.60	0.46	0.64	59	3.7	35.2
	SE	4.62	**0.49**	0.66	56	3.5	35.8
Gemma	ZS	4.10	0.30	0.45	70	4.8	33.0
	FS	4.30	0.32	0.46	68	4.6	33.5
	CoT	4.32	0.33	0.47	65	4.4	34.0
	SE	4.35	0.34	0.48	62	4.2	34.5
LLaVA	ZS	4.00	0.28	0.42	140	6.7	30.0
	FS	4.05	0.29	0.43	135	6.5	30.2
	CoT	4.10	0.30	0.44	130	6.2	30.5
	SE	4.15	0.32	0.45	125	5.2	33.3
LLaMA	ZS	4.14	0.31	0.46	66	4.9	34.0
	FS	4.25	0.32	0.47	64	4.7	34.5
	COT	4.28	0.34	0.48	62	4.5	35.0
	SE	4.32	0.35	0.49	60	4.4	35.5
Qwen	ZS	**4.27**	0.29	0.44	72	4.2	33.5
	FS	4.45	0.30	0.45	68	4.0	34.2
	COT	4.50	0.32	0.46	66	3.8	34.8
	SE	4.55	0.33	0.47	64	3.7	35.2

Table 2: Reference-Free Evaluation of Models on **SMARTEdit-Bench-Posters**.

System	EA ↑	DL ↑	SM ↑	Overlap ↑
DALLE-3	3.95	3.75	4.10	3.55
InstructPix2Pix	3.85	3.40	3.90	3.65
HIVE	4.00	3.60	4.00	4.00
Gligen + Reward-Refine	4.28	4.10	4.32	4.15
Gligen + RewardDPO	**4.35**	**4.20**	**4.40**	**4.25**
Gold Image	4.50	4.50	4.50	4.50

Table 3: GPT-4o-based evaluation of image edits on **SMARTEdit-Bench** – Natural Images (1-5). EA = Edit Adherence (instruction following), DL = Depth Layering, SM = Semantic Match (via CLIP), Overlap = Visual realism in size and placement.

5 Experimental Setup and Main Results

We aim to assess whether layout and content generated by LLMs/VLMs after edit instruction are "smart" enough and we benchmark the model's capabilities along various dimensions. Besides, we also check how much performance boost has been made by our proposed **SMART-Editor**. To this end, we structure our experiments as below:

5.1 How "smart" are the edits made by the base models compared to SMART-Editor?

We evaluate the 'smartness' of LLMs and VLMs to perform layout and semantic content editing in line with human design principles. Our experiments include three LLMs—**Gemma** (Team et al., 2024b), **LLaMA** (Touvron et al., 2023), and

Qwen (Bai et al., 2023)—and three VLMs—**GPT-4o** (OpenAI et al., 2024), **Gemini-Pro** (Team et al., 2024a), and **LLaVA** (Liu et al., 2023)—each evaluated under four inference settings: **Zero-Shot (ZS)**, **Few-Shot (FS)**, **Chain-of-Thought (CoT)**, and **SMART-Editor Reward-Refine (SE)** (Appendix 12.5 for prompts, inference settings and HuggingFace-Models). All three LLMs and three VLMs contribute to generating layout edits in the SMART-Editor's Reward-Refine variant across all domains, while only LLMs are employed in the RewardDPO-based fine-tuning setup (Finetuning details in Appendix 12.6). When the instruction involves semantic content modification (i.e., action: `updatetext`), we delegate content generation exclusively to **GPT-4o**, which identifies target regions and rewrites content for specific sections accordingly. For unstructured image domains, we retain GPT-4o for textual grounding and use state-of-the-art **GLIGEN** (Li et al., 2023) to synthesize updated visuals within specified object bounding boxes.

For structured domains, we use LayoutPrompter (Shi et al., 2025) as the state-of-the-art training-free baseline to compare the 'smartness' of edits when evaluating on the human-created posters and websites. For natural images, we consider the following latest image-editing baselines: a) Instructpix2pix (Brooks et al., 2023) b) DALLE-3 (Danescu-Niculescu-Mizil et al., 2012), c) HIVE (Zhang et al., 2024b).

Evaluation Setup. We evaluate the quality of editing across both **structured domains** (e.g., posters, webpages) and **unstructured domains** (e.g., natural images) using a combination of **reference-free** and **reference-based** methods (Evaluation methods in Appendix 12.1, 12.2, 12.3)

Reference-Free Takeaways. Tables 2 and 18 present the performance of LLMs and VLMs on **SMARTEdit-Bench-Posters** and **SMARTEdit-Bench-Websites** respectively. On **SMARTEdit-Bench-Posters**, while the zero-shot, few-shot, CoT variants struggle, GPT-4o (Reward-Refine) achieves the best layout editing performance—edit adherence 4.70, cross-section consistency 0.67, and alignment 36.5—outperforming LayoutPrompter. Gemini-Pro also shows notable gains with refinement. On **SMARTEdit-Bench-Websites**, layout editing is more challenging, but SMART-Editor still improves results: GPT-4o (Reward-Refine) leads with cross-section score 0.66, lower overlap

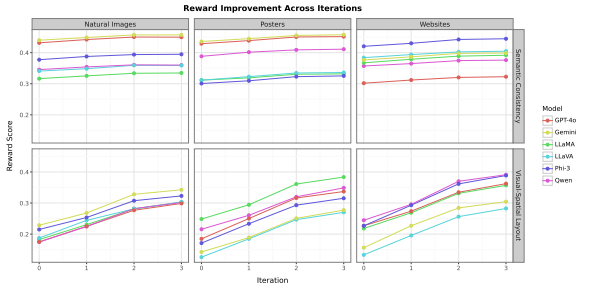

Figure 3: Reward improvement over iterations across semantic and visual dimensions on the posters, websites and natural images. Semantic consistency shows minimal gains across iterations for natural images, while visual-spatial layout rewards improve more sharply for posters and websites.

Figure 4: Models trained with RewardDPO and refined using Reward-Refine achieve higher composite rewards—reflecting better semantic and spatial layout quality—compared to SFT and Zero-Shot baselines.

(70), and higher alignment (31.5), demonstrating robust spatial understanding.

Reference-Based Takeaways. On **SMARTEdit-Bench-Posters**, GPT-4o + Reward-Refine achieves the highest layout similarity (4.47) and strong semantic consistency (4.38), outperforming LayoutPrompter (4.01). RewardDPO fine-tuning also boosts LLaMA and Gemma by +0.22 in layout alignment (Table 12). On **SMARTEdit-Bench-Websites**, GPT-4o + Reward-Refine again leads with LS = 4.45 (+0.45) and SC = 4.50. Gemini-Pro shows consistent gains (LS = 4.36, SC = 4.32), highlighting the benefit of reward-based refinement (Table 17). On **SMARTEdit-Bench** – Natural Images, Gligen + RewardDPO achieves near-gold scores (4.35–4.40) across all axes—edit adherence, depth layering, semantic match, and realism—outperforming DALLE-3, HIVE, and InstructPix2Pix (Table 3).

Impact of Edit Types. To pinpoint specific weaknesses in model reasoning, we analyze the model behavior under four common edit operations—*Insert*, *Delete*, *Reordering*, and *Content Grouping*—by measuring reward deltas between

Edit Type	Narrative ↓	Layout ↓	Cross-Section Consistency ↓
Insert	-12.3%	**-17.6%**	-0.22%
Delete	-10.0%	**-14.4%**	-0.12%
Reordering	-0.08%	**-15.9%**	0%
Content Grouping	-0.12%	**-12.7%**	0%

Table 4: Average relative reward drop across reasoning dimensions by edit type (from zero-shot baseline). Layout degradation dominates across Insert, Delete, and Grouping edits, followed by narrative incoherence. Cross-section consistency is relatively more preserved.

Model A vs. B	Posters	Websites	Natural Images
RewardDPO vs. LayoutPrompter	65.4%	72.1%	-
Reward-Refine vs. HIVE	-	-	78.2%
RewardDPO vs. Reward-Refine	**82.5%**	**78.6%**	48.2%
RewardDPO vs. SFT	**88.6%**	**84.3%**	78.2%
RewardDPO vs. Zero-Shot	**95.5%**	**93.7%**	90.0%
Reward-Refine vs. SFT	63.2%	67.5%	**80.4%**
Reward-Refine vs. Zero-Shot	84.7%	87.0%	**92.1%**
SFT vs. Zero-Shot	61.8%	68.2%	69.5%

Table 5: WTR from human preference rankings, reported for Posters, Websites, and Natural Images (Base-LLama). RewardDPO is preferred in structured domains; Reward-Refine performs best in natural scenes.

Ablation	EA ↑	NC ↑	Overlap ↓	Algn ↑
Reward-Refine (Full)	4.40	0.41	-62.0	33.2
A1: – Reward Replanning	4.22	0.35	-71.0	30.0
A2: – Language Feedback	4.28	0.33	-66.5	31.2
RewardDPO (Full)	4.55	0.44	-58.0	34.0
A3: – Rand Negatives (RandNeg)	4.42	0.37	-66.0	31.5
A4: – No Reward Filtering	4.40	0.39	-63.5	32.0

Table 6: Ablation results across all domains (average). Both Reward-Refine and RewardDPO rely heavily on reward-driven structure: removing reward-based replanning or curated preference data harms performance.

pre-edit and post-edits. Results (Table 4) reveal that layout reward is most sensitive, with severe degradation from *Insert* (17.6%) and *Reordering* (15.9%) edits due to increased overlap and whitespace. Narrative coherence also drops sharply under *Insert* (12.3%) and *Delete* (10.0%) due to unbalanced or contextless updates. In contrast, *Cross-Sectional Consistency* is minimally affected (-0.22%), suggesting models better preserve high-level structural alignment than local spatial or narrative coherence.

Reward-Refine vs RewardDPO. We compare RewardDPO with Zero-Shot, Supervised Finetuning (SFT), and Reward-Refine (Figure 4) for all the LLMs in **SMART-Editor**. Across all models and domains, RewardDPO achieves the highest composite rewards, indicating better alignment with semantic and visual-spatial layout goals. While Reward-Refine improves quality through iterative correction, RewardDPO matches or exceeds its final performance with greater efficiency. Gains are strongest in structured domains like posters and websites, where layout feedback is explicit. In natural images, improvements are modest, suggesting that while RewardDPO optimizes structural edits well, semantic reasoning in unstructured scenes still remains a challenge.

5.2 Ablation Analysis in SMART-Editor

Impact of Iterations in Reward-Refine. To assess how well models improve layout and content over time, we apply **Reward-Refine** across natural images, posters, and websites, iteratively updating model outputs using composite reward feedback as summation of metric scores (Details in Appendix 12.4). Each round optimizes two key reasoning dimensions: semantic consistency and visual-spatial layout. As shown in Figure 3, most visual-spatial improvements occur within the first two iterations—especially in structured domains like posters and websites—driven by alignment and spacing feedback. Semantic gains are slower and often plateau. In natural image editing, it helps bridge perceptual gaps in occlusion, depth layering, and instruction adherence, outperforming traditional baselines (Table 3).

Impact of Components in SMART-Editor. To better understand the contribution of individual components, we conduct targeted ablation studies across posters, websites, and natural images (Table 6). Each ablation selectively removes a key mechanism from either Reward-Refine or RewardDPO. **A1: No Reward-Based Replanning (Reward-Refine)** We disable iterative reward-guided refinement and use only initial layout edits to test whether passive edits suffice; this leads to a 9–11 point drop in layout quality, showing that structured edits require active spatial reasoning. **A2: No Language Feedback (Reward-Refine)** We remove intermediate natural language feedback prompts to assess their role in guiding semantic fixes; as a result, semantic consistency, especially in natural images, degrades due to lack of localized corrective signals. **A3: Random Negatives (RewardDPO)** We substitute structured corrupted pairs with random preferences during DPO training to test learning signal specificity; this weakens narrative and alignment understanding, resulting in incoherent section ordering and poor layout structure. **A4: No Reward Filtering (Reward-DPO)** We skip the step of filtering preference pairs based on reward alignment to see how noise affects preference modeling; this introduces contradictory

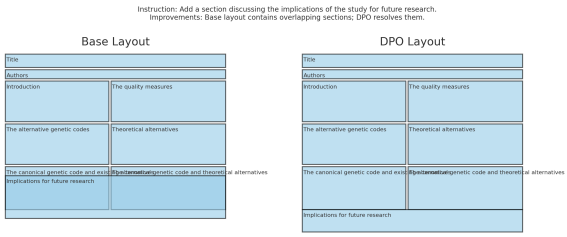

Figure 5: Poster edit example: RewardDPO fixes overlap and restores alignment after inserting a new section.

supervision, reducing the model's ability to align edits with the intended quality axes. Additionally, we also perform ablation on the impact of training data in RewardDPO and the impact of critics (Appendix 13.1, 13.2, 13.3).

5.3 Human Evaluation

We run human evaluation (Instructions in Figure 12) across posters, websites, and natural images, comparing four model variants: Zero-Shot, SFT, Reward-Refine, and RewardDPO. Annotators rank outputs based on edit quality given an instruction and initial layout. Using win–tie–rate (WTR) statistics from 30 samples per domain, we observe that **RewardDPO and Reward-Refine consistently outperform baselines** (Table 5). In posters and websites, RewardDPO dominates Reward-Refine in over 78% of pairwise comparisons, confirming the value of reward-aligned learning in structured settings. For natural images, Reward-Refine slightly edges out RewardDPO (51.8%), suggesting iterative feedback better captures visual plausibility. Both methods strongly outperform SFT and Zero-Shot across all domains.

5.4 Qualitative Case Studies

We present qualitative case studies across structured and unstructured domains to highlight the effectiveness of SMART-Editor. In Figure 5, RewardDPO resolves layout overlap and restores alignment after inserting a new section in a scientific poster, while Figure 6 shows Reward-Refine reshuffling a webpage layout to improve narrative coherence and spatial usability. For natural images (Figure 9), GLIGEN with RewardDPO accurately transforms a rainforest scene into an arctic landscape with polar bears; in contrast, InstructPix2Pix fails to remove the parrot or reflect the scene semantics (Figure 8).

6 Related Work

Our work lies at the intersection of instruction-based editing, structured layout modeling, and com-

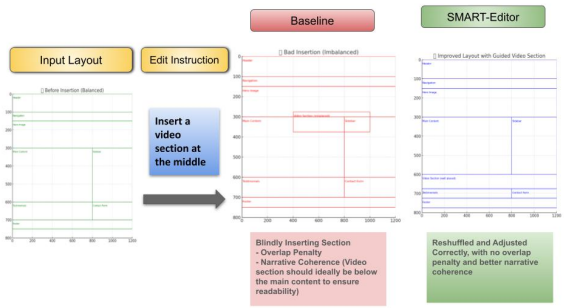

Figure 6: Webpage Edit example: Reward-Refine successfully improves spatial arrangement and UX goals based on the insert instruction.

positional reasoning. Instruction-guided image editing approaches like InstructPix2Pix (Brooks et al., 2023), HumanEdit (Bai et al., 2025), and HQ-Edit (Hui et al., 2024) focus on pixel-level transformations but largely ignore how edits propagate through structured scenes. While these models improve visual realism, they lack mechanisms to reason over cascading changes in layout or content coherence. In the structured domain, models such as LayoutGAN (Li et al., 2019), LayoutTransformer (Chai et al., 2023), and LayoutGPT (Feng et al., 2023b) synthesize layouts from scratch but do not support iterative editing or reward-based refinement. Recent work like LayoutCoT (Shi et al., 2025) brings reasoning into layout generation but lacks evaluation of edit propagation. Benchmarks such as SciPostLayout (Tanaka et al., 2024) and InstructEdit (Wang et al., 2023) support layout understanding, but not compositional edit evaluation. Programmatic editing in code (Fried et al., 2023) and HTML (Li et al., 2022) explores instruction-following with symbolic reasoning, which inspires our approach to layout action planning. However, these systems operate in text/code domains and lack alignment with visual-semantic layout structures. Unlike prior work, we focus on whether edits preserve global structure (More in Appendix 10).

7 Conclusion and Future Work

This work introduces SMART-Editor, a unified framework for layout and scene editing that emphasizes design integrity. By combining inference-time refinement and training-time preference optimization, SMART-Editor achieves significant improvements in both structured and unstructured domains. Moving forward, we envision extending SMART-Editor to multi-turn editing, and real-world human-in-the-loop design workflows.

Limitations

- **Assumption of Reliable Rewards:** Reward-Refine assumes access to well-defined, reliable reward functions. In real-world design workflows, such signals may be noisy, latent, or subjective.
- **Single-Turn Editing Focus:** Our framework is evaluated on isolated editing instructions. Multi-turn, interactive layout editing remains unexplored and may require modeling user intent over time.
- **Inference-Time Overhead:** Reward-Refine improves output quality but incurs additional computational cost during inference and may be sensitive to initialization or local optima.

Ethics Statement

The experiments performed in this study involved human participants. All the experiments involving human evaluation were exempt under institutional IRB review. We recruited participants for our human study using Upwork and we have fairly compensated all the Upwork freelancers involved in this study, at an average rate of 15.00 USD per hour (respecting their suggested Upwork hourly wage). We did not collect any personal data during the experiments, and they could choose not to participate in the study. The documents used in the study are distributed under an open license.

While this work adheres to ethical guidelines for human participation and open data usage, it presents some potential risks. First, automated layout modifications—especially in scientific or web-based content—may unintentionally alter the intended communicative structure or introduce misinformation if misused. Second, systems that rely on implicit, instruction-based editing could generate plausible but incorrect edits that are difficult to verify without human oversight, potentially reducing user trust. Finally, the deployment of such editing systems in real-world design workflows without adequate guardrails may diminish creative control.

References

Jinbin Bai, Wei Chow, Ling Yang, Xiangtai Li, Juncheng Li, Hanwang Zhang, and Shuicheng Yan. 2025. Humanedit: A high-quality human-rewarded dataset for instruction-based image editing. *Preprint*, arXiv:2412.04280.

Jinze Bai, Shuai Bai, Yunfei Chu, Zeyu Cui, Kai Dang, Xiaodong Deng, Yang Fan, Wenbin Ge, Yu Han, Fei Huang, Binyuan Hui, Luo Ji, Mei Li, Junyang Lin, Runji Lin, Dayiheng Liu, Gao Liu, Chengqiang Lu, Keming Lu, Jianxin Ma, Rui Men, Xingzhang Ren, Xuancheng Ren, Chuanqi Tan, Sinan Tan, Jianhong Tu, Peng Wang, Shijie Wang, Wei Wang, Shengguang Wu, Benfeng Xu, Jin Xu, An Yang, Hao Yang, Jian Yang, Shusheng Yang, Yang Yao, Bowen Yu, Hongyi Yuan, Zheng Yuan, Jianwei Zhang, Xingxuan Zhang, Yichang Zhang, Zhenru Zhang, Chang Zhou, Jingren Zhou, Xiaohuan Zhou, and Tianhang Zhu. 2023. Qwen technical report. *Preprint*, arXiv:2309.16609.

Tim Brooks, Aleksander Holynski, and Alexei A. Efros. 2023. Instructpix2pix: Learning to follow image editing instructions. *Preprint*, arXiv:2211.09800.

Shang Chai, Liansheng Zhuang, and Fengying Yan. 2023. Layoutdm: Transformer-based diffusion model for layout generation. *Preprint*, arXiv:2305.02567.

Mark Chen, Jerry Tworek, Heewoo Jun, Qiming Yuan, Henrique Ponde de Oliveira Pinto, Jared Kaplan, Harri Edwards, Yuri Burda, Nicholas Joseph, Greg Brockman, Alex Ray, Raul Puri, Gretchen Krueger, Michael Petrov, Heidy Khlaaf, Girish Sastry, Pamela Mishkin, Brooke Chan, Scott Gray, Nick Ryder, Mikhail Pavlov, Alethea Power, Lukasz Kaiser, Mohammad Bavarian, Clemens Winter, Philippe Tillet, Felipe Petroski Such, Dave Cummings, Matthias Plappert, Fotios Chantzis, Elizabeth Barnes, Ariel Herbert-Voss, William Hebgen Guss, Alex Nichol, Alex Paino, Nikolas Tezak, Jie Tang, Igor Babuschkin, Suchir Balaji, Shantanu Jain, William Saunders, Christopher Hesse, Andrew N. Carr, Jan Leike, Josh Achiam, Vedant Misra, Evan Morikawa, Alec Radford, Matthew Knight, Miles Brundage, Mira Murati, Katie Mayer, Peter Welinder, Bob McGrew, Dario Amodei, Sam McCandlish, Ilya Sutskever, and Wojciech Zaremba. 2021. Evaluating large language models trained on code. *Preprint*, arXiv:2107.03374.

Cristian Danescu-Niculescu-Mizil, Lillian Lee, Bo Pang, and Jon Kleinberg. 2012. Echoes of power: Language effects and power differences in social interaction. In *Proceedings of WWW*, pages 699–708.

Weixi Feng, Wanrong Zhu, Tsu-jui Fu, Varun Jampani, Arjun Akula, Xuehai He, Sugato Basu, Xin Eric Wang, and William Yang Wang. 2023a. Layoutgpt: compositional visual planning and generation with large language models. In *Proceedings of the 37th International Conference on Neural Information Processing Systems*, NIPS '23, Red Hook, NY, USA. Curran Associates Inc.

Weixi Feng, Wanrong Zhu, Tsu jui Fu, Varun Jampani, Arjun Akula, Xuehai He, Sugato Basu, Xin Eric Wang, and William Yang Wang. 2023b. Layoutgpt: Compositional visual planning and generation with large language models. *Preprint*, arXiv:2305.15393.

Daniel Fried, Armen Aghajanyan, Jessy Lin, Sida Wang, Eric Wallace, Freda Shi, Ruiqi Zhong, Wen tau Yih, Luke Zettlemoyer, and Mike Lewis. 2023. Incoder: A generative model for code infilling and synthesis. *Preprint*, arXiv:2204.05999.

Hanan Gani, Shariq Farooq Bhat, Muzammal Naseer, Salman Khan, and Peter Wonka. 2024. Llm blueprint: Enabling text-to-image generation with complex and detailed prompts. *Preprint*, arXiv:2310.10640.

Yuying Ge, Sijie Zhao, Chen Li, Yixiao Ge, and Ying Shan. 2024. Seed-data-edit technical report: A hybrid dataset for instructional image editing. *Preprint*, arXiv:2405.04007.

Claire Golomb. 1987. The development of compositional strategies in children's drawings. *Visual Arts Research*, pages 42–52.

Mude Hui, Siwei Yang, Bingchen Zhao, Yichun Shi, Heng Wang, Peng Wang, Yuyin Zhou, and Cihang Xie. 2024. Hq-edit: A high-quality dataset for instruction-based image editing. *Preprint*, arXiv:2404.09990.

Peidong Jia, Chenxuan Li, Yuhui Yuan, Zeyu Liu, Yichao Shen, Bohan Chen, Xingru Chen, Yinglin Zheng, Dong Chen, Ji Li, Xiaodong Xie, Shanghang Zhang, and Baining Guo. 2024. Cole: A hierarchical generation framework for multi-layered and editable graphic design. *Preprint*, arXiv:2311.16974.

Akash Abdu Jyothi, Thibaut Durand, Jiawei He, Leonid Sigal, and Greg Mori. 2021. Layoutvae: Stochastic scene layout generation from a label set. *Preprint*, arXiv:1907.10719.

Alexander Kirillov, Eric Mintun, Nikhila Ravi, Hanzi Mao, Chloe Rolland, Laura Gustafson, Tete Xiao, Spencer Whitehead, Alexander C. Berg, Wan-Yen Lo, Piotr Dollár, and Ross Girshick. 2023. Segment anything. *Preprint*, arXiv:2304.02643.

Jianan Li, Jimei Yang, Aaron Hertzmann, Jianming Zhang, and Tingfa Xu. 2019. Layoutgan: Generating graphic layouts with wireframe discriminators. *Preprint*, arXiv:1901.06767.

Jingyu Li, Wei Liu, and Tan Lee. 2022. Editnet: A lightweight network for unsupervised domain adaptation in speaker verification. *Preprint*, arXiv:2206.07548.

Yuheng Li, Haotian Liu, Qingyang Wu, Fangzhou Mu, Jianwei Yang, Jianfeng Gao, Chunyuan Li, and Yong Jae Lee. 2023. Gligen: Open-set grounded text-to-image generation. *Preprint*, arXiv:2301.07093.

Jiawei Lin, Jiaqi Guo, Shizhao Sun, Zijiang James Yang, Jian-Guang Lou, and Dongmei Zhang. 2023. Layoutprompter: Awaken the design ability of large language models. *Preprint*, arXiv:2311.06495.

Yuanze Lin, Yi-Wen Chen, Yi-Hsuan Tsai, Lu Jiang, and Ming-Hsuan Yang. 2024. Text-driven image editing via learnable regions. In *Proceedings of the IEEE/CVF Conference on Computer Vision and Pattern Recognition (CVPR)*, pages 7059–7068.

Haotian Liu, Chunyuan Li, Qingyang Wu, and Yong Jae Lee. 2023. Visual instruction tuning. *Preprint*, arXiv:2304.08485.

George A Lozano. 2014. Ethics of using language editing services in an era of digital communication and heavily multi-authored papers. *Science and Engineering Ethics*, 20(2):363–377.

OpenAI, Josh Achiam, Steven Adler, Sandhini Agarwal, Lama Ahmad, Ilge Akkaya, Florencia Leoni Aleman, Diogo Almeida, Janko Altenschmidt, Sam Altman, Shyamal Anadkat, Red Avila, Igor Babuschkin, Suchir Balaji, Valerie Balcom, Paul Baltescu, Haiming Bao, Mohammad Bavarian, Jeff Belgum, Irwan Bello, Jake Berdine, Gabriel Bernadett-Shapiro, Christopher Berner, Lenny Bogdonoff, Oleg Boiko, Madelaine Boyd, Anna-Luisa Brakman, Greg Brockman, Tim Brooks, Miles Brundage, Kevin Button, Trevor Cai, Rosie Campbell, Andrew Cann, Brittany Carey, Chelsea Carlson, Rory Carmichael, Brooke Chan, Che Chang, Fotis Chantzis, Derek Chen, Sully Chen, Ruby Chen, Jason Chen, Mark Chen, Ben Chess, Chester Cho, Casey Chu, Hyung Won Chung, Dave Cummings, Jeremiah Currier, Yunxing Dai, Cory Decareaux, Thomas Degry, Noah Deutsch, Damien Deville, Arka Dhar, David Dohan, Steve Dowling, Sheila Dunning, Adrien Ecoffet, Atty Eleti, Tyna Eloundou, David Farhi, Liam Fedus, Niko Felix, Simón Posada Fishman, Juston Forte, Isabella Fulford, Leo Gao, Elie Georges, Christian Gibson, Vik Goel, Tarun Gogineni, Gabriel Goh, Rapha Gontijo-Lopes, Jonathan Gordon, Morgan Grafstein, Scott Gray, Ryan Greene, Joshua Gross, Shixiang Shane Gu, Yufei Guo, Chris Hallacy, Jesse Han, Jeff Harris, Yuchen He, Mike Heaton, Johannes Heidecke, Chris Hesse, Alan Hickey, Wade Hickey, Peter Hoeschele, Brandon Houghton, Kenny Hsu, Shengli Hu, Xin Hu, Joost Huizinga, Shantanu Jain, Shawn Jain, Joanne Jang, Angela Jiang, Roger Jiang, Haozhun Jin, Denny Jin, Shino Jomoto, Billie Jonn, Heewoo Jun, Tomer Kaftan, Łukasz Kaiser, Ali Kamali, Ingmar Kanitscheider, Nitish Shirish Keskar, Tabarak Khan, Logan Kilpatrick, Jong Wook Kim, Christina Kim, Yongjik Kim, Jan Hendrik Kirchner, Jamie Kiros, Matt Knight, Daniel Kokotajlo, Łukasz Kondraciuk, Andrew Kondrich, Aris Konstantinidis, Kyle Kosic, Gretchen Krueger, Vishal Kuo, Michael Lampe, Ikai Lan, Teddy Lee, Jan Leike, Jade Leung, Daniel Levy, Chak Ming Li, Rachel Lim, Molly Lin, Stephanie Lin, Mateusz Litwin, Theresa Lopez, Ryan Lowe, Patricia Lue, Anna Makanju, Kim Malfacini, Sam Manning, Todor Markov, Yaniv Markovski, Bianca Martin, Katie Mayer, Andrew Mayne, Bob McGrew, Scott Mayer McKinney, Christine McLeavey, Paul McMillan, Jake McNeil, David Medina, Aalok Mehta, Jacob Menick, Luke Metz, Andrey Mishchenko, Pamela

Mishkin, Vinnie Monaco, Evan Morikawa, Daniel Mossing, Tong Mu, Mira Murati, Oleg Murk, David Mély, Ashvin Nair, Reiichiro Nakano, Rajeev Nayak, Arvind Neelakantan, Richard Ngo, Hyeonwoo Noh, Long Ouyang, Cullen O'Keefe, Jakub Pachocki, Alex Paino, Joe Palermo, Ashley Pantuliano, Giambattista Parascandolo, Joel Parish, Emy Parparita, Alex Passos, Mikhail Pavlov, Andrew Peng, Adam Perelman, Filipe de Avila Belbute Peres, Michael Petrov, Henrique Ponde de Oliveira Pinto, Michael, Pokorny, Michelle Pokrass, Vitchyr H. Pong, Tolly Powell, Alethea Power, Boris Power, Elizabeth Proehl, Raul Puri, Alec Radford, Jack Rae, Aditya Ramesh, Cameron Raymond, Francis Real, Kendra Rimbach, Carl Ross, Bob Rotsted, Henri Roussez, Nick Ryder, Mario Saltarelli, Ted Sanders, Shibani Santurkar, Girish Sastry, Heather Schmidt, David Schnurr, John Schulman, Daniel Selsam, Kyla Sheppard, Toki Sherbakov, Jessica Shieh, Sarah Shoker, Pranav Shyam, Szymon Sidor, Eric Sigler, Maddie Simens, Jordan Sitkin, Katarina Slama, Ian Sohl, Benjamin Sokolowsky, Yang Song, Natalie Staudacher, Felipe Petroski Such, Natalie Summers, Ilya Sutskever, Jie Tang, Nikolas Tezak, Madeleine B. Thompson, Phil Tillet, Amin Tootoonchian, Elizabeth Tseng, Preston Tuggle, Nick Turley, Jerry Tworek, Juan Felipe Cerón Uribe, Andrea Vallone, Arun Vijayvergiya, Chelsea Voss, Carroll Wainwright, Justin Jay Wang, Alvin Wang, Ben Wang, Jonathan Ward, Jason Wei, CJ Weinmann, Akila Welihinda, Peter Welinder, Jiayi Weng, Lilian Weng, Matt Wiethoff, Dave Willner, Clemens Winter, Samuel Wolrich, Hannah Wong, Lauren Workman, Sherwin Wu, Jeff Wu, Michael Wu, Kai Xiao, Tao Xu, Sarah Yoo, Kevin Yu, Qiming Yuan, Wojciech Zaremba, Rowan Zellers, Chong Zhang, Marvin Zhang, Shengjia Zhao, Tianhao Zheng, Juntang Zhuang, William Zhuk, and Barret Zoph. 2024. Gpt-4 technical report. *Preprint*, arXiv:2303.08774.

Alec Radford, Jong Wook Kim, Chris Hallacy, Aditya Ramesh, Gabriel Goh, Sandhini Agarwal, Girish Sastry, Amanda Askell, Pamela Mishkin, Jack Clark, Gretchen Krueger, and Ilya Sutskever. 2021. Learning transferable visual models from natural language supervision. *Preprint*, arXiv:2103.00020.

Rafael Rafailov, Archit Sharma, Eric Mitchell, Stefano Ermon, Christopher D. Manning, and Chelsea Finn. 2024. Direct preference optimization: Your language model is secretly a reward model. *Preprint*, arXiv:2305.18290.

Tianhe Ren, Qing Jiang, Shilong Liu, Zhaoyang Zeng, Wenlong Liu, Han Gao, Hongjie Huang, Zhengyu Ma, Xiaoke Jiang, Yihao Chen, Yuda Xiong, Hao Zhang, Feng Li, Peijun Tang, Kent Yu, and Lei Zhang. 2024. Grounding dino 1.5: Advance the "edge" of open-set object detection. *Preprint*, arXiv:2405.10300.

Hengyu Shi, Junhao Su, Huansheng Ning, Xiaoming Wei, and Jialin Gao. 2025. Layoutcot: Unleashing the deep reasoning potential of large language models for layout generation. *Preprint*, arXiv:2504.10829.

Chenglei Si, Yanzhe Zhang, Ryan Li, Zhengyuan Yang, Ruibo Liu, and Diyi Yang. 2025. Design2Code: Benchmarking multimodal code generation for automated front-end engineering. In *Proceedings of the 2025 Conference of the Nations of the Americas Chapter of the Association for Computational Linguistics: Human Language Technologies (Volume 1: Long Papers)*, pages 3956–3974, Albuquerque, New Mexico. Association for Computational Linguistics.

Manan Suri, Puneet Mathur, Franck Dernoncourt, Rajiv Jain, Vlad I Morariu, Ramit Sawhney, Preslav Nakov, and Dinesh Manocha. 2024. DocEdit-v2: Document structure editing via multimodal LLM grounding. In *Proceedings of the 2024 Conference on Empirical Methods in Natural Language Processing*, pages 15485–15505, Miami, Florida, USA. Association for Computational Linguistics.

Shohei Tanaka, Hao Wang, and Yoshitaka Ushiku. 2024. Scipostlayout: A dataset for layout analysis and layout generation of scientific posters. *Preprint*, arXiv:2407.19787.

Gemini Team, Petko Georgiev, Ving Ian Lei, Ryan Burnell, Libin Bai, Anmol Gulati, Garrett Tanzer, Damien Vincent, Zhufeng Pan, Shibo Wang, Soroosh Mariooryad, Yifan Ding, Xinyang Geng, Fred Alcober, Roy Frostig, Mark Omernick, Lexi Walker, Cosmin Paduraru, Christina Sorokin, Andrea Tacchetti, Colin Gaffney, Samira Daruki, Olcan Sercinoglu, Zach Gleicher, Juliette Love, Paul Voigtlaender, Rohan Jain, Gabriela Surita, Kareem Mohamed, Rory Blevins, Junwhan Ahn, Tao Zhu, Kornraphop Kawintiranon, Orhan Firat, Yiming Gu, Yujing Zhang, Matthew Rahtz, Manaal Faruqui, Natalie Clay, Justin Gilmer, JD Co-Reyes, Ivo Penchev, Rui Zhu, Nobuyuki Morioka, Kevin Hui, Krishna Haridasan, Victor Campos, Mahdis Mahdieh, Mandy Guo, Samer Hassan, Kevin Kilgour, Arpi Vezer, Heng-Tze Cheng, Raoul de Liedekerke, Siddharth Goyal, Paul Barham, DJ Strouse, Seb Noury, Jonas Adler, Mukund Sundararajan, Sharad Vikram, Dmitry Lepikhin, Michela Paganini, Xavier Garcia, Fan Yang, Dasha Valter, Maja Trebacz, Kiran Vodrahalli, Chulayuth Asawaroengchai, Roman Ring, Norbert Kalb, Livio Baldini Soares, Siddhartha Brahma, David Steiner, Tianhe Yu, Fabian Mentzer, Antoine He, Lucas Gonzalez, Bibo Xu, Raphael Lopez Kaufman, Laurent El Shafey, Junhyuk Oh, Tom Hennigan, George van den Driessche, Seth Odoom, Mario Lucic, Becca Roelofs, Sid Lall, Amit Marathe, Betty Chan, Santiago Ontanon, Luheng He, Denis Teplyashin, Jonathan Lai, Phil Crone, Bogdan Damoc, Lewis Ho, Sebastian Riedel, Karel Lenc, Chih-Kuan Yeh, Aakanksha Chowdhery, Yang Xu, Mehran Kazemi, Ehsan Amid, Anastasia Petrushkina, Kevin Swersky, Ali Khodaei, Gowoon Chen, Chris Larkin, Mario Pinto, Geng Yan, Adria Puigdomenech Badia, Piyush Patil, Steven Hansen, Dave Orr, Sebastien M. R. Arnold, Jordan Grimstad, Andrew Dai, Sholto Douglas, Rishika Sinha, Vikas Yadav, Xi Chen, Elena Gribovskaya, Jacob Austin, Jeffrey Zhao, Kaushal Patel, Paul Komarek, Sophia Austin, Sebastian Borgeaud,

Linda Friso, Abhimanyu Goyal, Ben Caine, Kris Cao, Da-Woon Chung, Matthew Lamm, Gabe Barth-Maron, Thais Kagohara, Kate Olszewska, Mia Chen, Kaushik Shivakumar, Rishabh Agarwal, Harshal Godhia, Ravi Rajwar, Javier Snaider, Xerxes Dotiwalla, Yuan Liu, Aditya Barua, Victor Ungureanu, Yuan Zhang, Bat-Orgil Batsaikhan, Mateo Wirth, James Qin, Ivo Danihelka, Tulsee Doshi, Martin Chadwick, Jilin Chen, Sanil Jain, Quoc Le, Arjun Kar, Madhu Gurumurthy, Cheng Li, Ruoxin Sang, Fangyu Liu, Lampros Lamprou, Rich Munoz, Nathan Lintz, Harsh Mehta, Heidi Howard, Malcolm Reynolds, Lora Aroyo, Quan Wang, Lorenzo Blanco, Albin Cassirer, Jordan Griffith, Dipanjan Das, Stephan Lee, Jakub Sygnowski, Zach Fisher, James Besley, Richard Powell, Zafarali Ahmed, Dominik Paulus, David Reitter, Zalan Borsos, Rishabh Joshi, Aedan Pope, Steven Hand, Vittorio Selo, Vihan Jain, Nikhil Sethi, Megha Goel, Takaki Makino, Rhys May, Zhen Yang, Johan Schalkwyk, Christina Butterfield, Anja Hauth, Alex Goldin, Will Hawkins, Evan Senter, Sergey Brin, Oliver Woodman, Marvin Ritter, Eric Noland, Minh Giang, Vijay Bolina, Lisa Lee, Tim Blyth, Ian Mackinnon, Machel Reid, Obaid Sarvana, David Silver, Alexander Chen, Lily Wang, Loren Maggiore, Oscar Chang, Nithya Attaluri, Gregory Thornton, Chung-Cheng Chiu, Oskar Bunyan, Nir Levine, Timothy Chung, Evgenii Eltyshev, Xiance Si, Timothy Lillicrap, Demetra Brady, Vaibhav Aggarwal, Boxi Wu, Yuanzhong Xu, Ross McIlroy, Kartikeya Badola, Paramjit Sandhu, Erica Moreira, Wojciech Stokowiec, Ross Hemsley, Dong Li, Alex Tudor, Pranav Shyam, Elahe Rahimtoroghi, Salem Haykal, Pablo Sprechmann, Xiang Zhou, Diana Mincu, Yujia Li, Ravi Addanki, Kalpesh Krishna, Xiao Wu, Alexandre Frechette, Matan Eyal, Allan Dafoe, Dave Lacey, Jay Whang, Thi Avrahami, Ye Zhang, Emanuel Taropa, Hanzhao Lin, Daniel Toyama, Eliza Rutherford, Motoki Sano, HyunJeong Choe, Alex Tomala, Chalence Safranek-Shrader, Nora Kassner, Mantas Pajarskas, Matt Harvey, Sean Sechrist, Meire Fortunato, Christina Lyu, Gamaleldin Elsayed, Chenkai Kuang, James Lottes, Eric Chu, Chao Jia, Chih-Wei Chen, Peter Humphreys, Kate Baumli, Connie Tao, Rajkumar Samuel, Cicero Nogueira dos Santos, Anders Andreassen, Nemanja Rakićević, Dominik Grewe, Aviral Kumar, Stephanie Winkler, Jonathan Caton, Andrew Brock, Sid Dalmia, Hannah Sheahan, Iain Barr, Yingjie Miao, Paul Natsev, Jacob Devlin, Feryal Behbahani, Flavien Prost, Yanhua Sun, Artiom Myaskovsky, Thanumalayan Sankaranarayana Pillai, Dan Hurt, Angeliki Lazaridou, Xi Xiong, Ce Zheng, Fabio Pardo, Xiaowei Li, Dan Horgan, Joe Stanton, Moran Ambar, Fei Xia, Alejandro Lince, Mingqiu Wang, Basil Mustafa, Albert Webson, Hyo Lee, Rohan Anil, Martin Wicke, Timothy Dozat, Abhishek Sinha, Enrique Piqueras, Elahe Dabir, Shyam Upadhyay, Anudhyan Boral, Lisa Anne Hendricks, Corey Fry, Josip Djolonga, Yi Su, Jake Walker, Jane Labanowski, Ronny Huang, Vedant Misra, Jeremy Chen, RJ Skerry-Ryan, Avi Singh, Shruti Rijhwani, Dian Yu, Alex Castro-Ros, Beer Changpinyo, Romina Datta, Sumit Bagri, Arnar Mar Hrafnkelsson, Marcello Maggioni, Daniel Zheng, Yury Sulsky, Shaobo Hou, Tom Le Paine, Antoine Yang, Jason Riesa, Dominika Rogozinska, Dror Marcus, Dalia El Badawy, Qiao Zhang, Luyu Wang, Helen Miller, Jeremy Greer, Lars Lowe Sjos, Azade Nova, Heiga Zen, Rahma Chaabouni, Mihaela Rosca, Jiepu Jiang, Charlie Chen, Ruibo Liu, Tara Sainath, Maxim Krikun, Alex Polozov, Jean-Baptiste Lespiau, Josh Newlan, Zeyncep Cankara, Soo Kwak, Yunhan Xu, Phil Chen, Andy Coenen, Clemens Meyer, Katerina Tsihlas, Ada Ma, Juraj Gottweis, Jinwei Xing, Chenjie Gu, Jin Miao, Christian Frank, Zeynep Cankara, Sanjay Ganapathy, Ishita Dasgupta, Steph Hughes-Fitt, Heng Chen, David Reid, Keran Rong, Hongmin Fan, Joost van Amersfoort, Vincent Zhuang, Aaron Cohen, Shixiang Shane Gu, Anhad Mohananey, Anastasija Ilic, Taylor Tobin, John Wieting, Anna Bortsova, Phoebe Thacker, Emma Wang, Emily Caveness, Justin Chiu, Eren Sezener, Alex Kaskasoli, Steven Baker, Katie Millican, Mohamed Elhawaty, Kostas Aisopos, Carl Lebsack, Nathan Byrd, Hanjun Dai, Wenhao Jia, Matthew Wiethoff, Elnaz Davoodi, Albert Weston, Lakshman Yagati, Arun Ahuja, Isabel Gao, Golan Pundak, Susan Zhang, Michael Azzam, Khe Chai Sim, Sergi Caelles, James Keeling, Abhanshu Sharma, Andy Swing, YaGuang Li, Chenxi Liu, Carrie Grimes Bostock, Yamini Bansal, Zachary Nado, Ankesh Anand, Josh Lipschultz, Abhijit Karmarkar, Lev Proleev, Abe Ittycheriah, Soheil Hassas Yeganeh, George Polovets, Aleksandra Faust, Jiao Sun, Alban Rrustemi, Pen Li, Rakesh Shivanna, Jeremiah Liu, Chris Welty, Federico Lebron, Anirudh Baddepudi, Sebastian Krause, Emilio Parisotto, Radu Soricut, Zheng Xu, Dawn Bloxwich, Melvin Johnson, Behnam Neyshabur, Justin Mao-Jones, Renshen Wang, Vinay Ramasesh, Zaheer Abbas, Arthur Guez, Constant Segal, Duc Dung Nguyen, James Svensson, Le Hou, Sarah York, Kieran Milan, Sophie Bridgers, Wiktor Gworek, Marco Tagliasacchi, James Lee-Thorp, Michael Chang, Alexey Guseynov, Ale Jakse Hartman, Michael Kwong, Ruizhe Zhao, Sheleem Kashem, Elizabeth Cole, Antoine Miech, Richard Tanburn, Mary Phuong, Filip Pavetic, Sebastien Cevey, Ramona Comanescu, Richard Ives, Sherry Yang, Cosmo Du, Bo Li, Zizhao Zhang, Mariko Iinuma, Clara Huiyi Hu, Aurko Roy, Shaan Bijwadia, Zhenkai Zhu, Danilo Martins, Rachel Saputro, Anita Gergely, Steven Zheng, Dawei Jia, Ioannis Antonoglou, Adam Sadovsky, Shane Gu, Yingying Bi, Alek Andreev, Sina Samangooei, Mina Khan, Tomas Kocisky, Angelos Filos, Chintu Kumar, Colton Bishop, Adams Yu, Sarah Hodkinson, Sid Mittal, Premal Shah, Alexandre Moufarek, Yong Cheng, Adam Bloniarz, Jaehoon Lee, Pedram Pejman, Paul Michel, Stephen Spencer, Vladimir Feinberg, Xuehan Xiong, Nikolay Savinov, Charlotte Smith, Siamak Shakeri, Dustin Tran, Mary Chesus, Bernd Bohnet, George Tucker, Tamara von Glehn, Carrie Muir, Yiran Mao, Hideto Kazawa, Ambrose Slone, Kedar Soparkar, Disha Shrivastava, James Cobon-Kerr, Michael Sharman, Jay Pavagadhi, Carlos Araya, Karolis Misiunas, Nimesh Ghelani,

Michael Laskin, David Barker, Qiujia Li, Anton Briukhov, Neil Houlsby, Mia Glaese, Balaji Lakshminarayanan, Nathan Schucher, Yunhao Tang, Eli Collins, Hyeontaek Lim, Fangxiaoyu Feng, Adria Recasens, Guangda Lai, Alberto Magni, Nicola De Cao, Aditya Siddhant, Zoe Ashwood, Jordi Orbay, Mostafa Dehghani, Jenny Brennan, Yifan He, Kelvin Xu, Yang Gao, Carl Saroufim, James Molloy, Xinyi Wu, Seb Arnold, Solomon Chang, Julian Schrittwieser, Elena Buchatskaya, Soroush Radpour, Martin Polacek, Skye Giordano, Ankur Bapna, Simon Tokumine, Vincent Hellendoorn, Thibault Sottiaux, Sarah Cogan, Aliaksei Severyn, Mohammad Saleh, Shantanu Thakoor, Laurent Shefey, Siyuan Qiao, Meenu Gaba, Shuo yiin Chang, Craig Swanson, Biao Zhang, Benjamin Lee, Paul Kishan Rubenstein, Gan Song, Tom Kwiatkowski, Anna Koop, Ajay Kannan, David Kao, Parker Schuh, Axel Stjerngren, Golnaz Ghiasi, Gena Gibson, Luke Vilnis, Ye Yuan, Felipe Tiengo Ferreira, Aishwarya Kamath, Ted Klimenko, Ken Franko, Kefan Xiao, Indro Bhattacharya, Miteyan Patel, Rui Wang, Alex Morris, Robin Strudel, Vivek Sharma, Peter Choy, Sayed Hadi Hashemi, Jessica Landon, Mara Finkelstein, Priya Jhakra, Justin Frye, Megan Barnes, Matthew Mauger, Dennis Daun, Khuslen Baatarsukh, Matthew Tung, Wael Farhan, Henryk Michalewski, Fabio Viola, Felix de Chaumont Quitry, Charline Le Lan, Tom Hudson, Qingze Wang, Felix Fischer, Ivy Zheng, Elspeth White, Anca Dragan, Jean baptiste Alayrac, Eric Ni, Alexander Pritzel, Adam Iwanicki, Michael Isard, Anna Bulanova, Lukas Zilka, Ethan Dyer, Devendra Sachan, Srivatsan Srinivasan, Hannah Muckenhirn, Honglong Cai, Amol Mandhane, Mukarram Tariq, Jack W. Rae, Gary Wang, Kareem Ayoub, Nicholas FitzGerald, Yao Zhao, Woohyun Han, Chris Alberti, Dan Garrette, Kashyap Krishnakumar, Mai Gimenez, Anselm Levskaya, Daniel Sohn, Josip Matak, Inaki Iturrate, Michael B. Chang, Jackie Xiang, Yuan Cao, Nishant Ranka, Geoff Brown, Adrian Hutter, Vahab Mirrokni, Nanxin Chen, Kaisheng Yao, Zoltan Egyed, Francois Galilee, Tyler Liechty, Praveen Kallakuri, Evan Palmer, Sanjay Ghemawat, Jasmine Liu, David Tao, Chloe Thornton, Tim Green, Mimi Jasarevic, Sharon Lin, Victor Cotruta, Yi-Xuan Tan, Noah Fiedel, Hongkun Yu, Ed Chi, Alexander Neitz, Jens Heitkaemper, Anu Sinha, Denny Zhou, Yi Sun, Charbel Kaed, Brice Hulse, Swaroop Mishra, Maria Georgaki, Sneha Kudugunta, Clement Farabet, Izhak Shafran, Daniel Vlasic, Anton Tsitsulin, Rajagopal Ananthanarayanan, Alen Carin, Guolong Su, Pei Sun, Shashank V, Gabriel Carvajal, Josef Broder, Iulia Comsa, Alena Repina, William Wong, Warren Weilun Chen, Peter Hawkins, Egor Filonov, Lucia Loher, Christoph Hirnschall, Weiyi Wang, Jingchen Ye, Andrea Burns, Hardie Cate, Diana Gage Wright, Federico Piccinini, Lei Zhang, Chu-Cheng Lin, Ionel Gog, Yana Kulizhskaya, Ashwin Sreevatsa, Shuang Song, Luis C. Cobo, Anand Iyer, Chetan Tekur, Guillermo Garrido, Zhuyun Xiao, Rupert Kemp, Huaixiu Steven Zheng, Hui Li, Ananth Agarwal, Christel Ngani, Kati Goshvadi, Rebeca Santamaria-Fernandez, Wojciech Fica, Xinyun Chen, Chris Gorgolewski, Sean Sun, Roopal Garg, Xinyu Ye, S. M. Ali Eslami, Nan Hua, Jon Simon, Pratik Joshi, Yelin Kim, Ian Tenney, Sahitya Potluri, Lam Nguyen Thiet, Quan Yuan, Florian Luisier, Alexandra Chronopoulou, Salvatore Scellato, Praveen Srinivasan, Minmin Chen, Vinod Koverkathu, Valentin Dalibard, Yaming Xu, Brennan Saeta, Keith Anderson, Thibault Sellam, Nick Fernando, Fantine Huot, Junehyuk Jung, Mani Varadarajan, Michael Quinn, Amit Raul, Maigo Le, Ruslan Habalov, Jon Clark, Komal Jalan, Kalesha Bullard, Achintya Singhal, Thang Luong, Boyu Wang, Sujeevan Rajayogam, Julian Eisenschlos, Johnson Jia, Daniel Finchelstein, Alex Yakubovich, Daniel Balle, Michael Fink, Sameer Agarwal, Jing Li, Dj Dvijotham, Shalini Pal, Kai Kang, Jaclyn Konzelmann, Jennifer Beattie, Olivier Dousse, Diane Wu, Remi Crocker, Chen Elkind, Siddhartha Reddy Jonnalagadda, Jong Lee, Dan Holtmann-Rice, Krystal Kallarackal, Rosanne Liu, Denis Vnukov, Neera Vats, Luca Invernizzi, Mohsen Jafari, Huanjie Zhou, Lilly Taylor, Jennifer Prendki, Marcus Wu, Tom Eccles, Tianqi Liu, Kavya Kopparapu, Francoise Beaufays, Christof Angermueller, Andreea Marzoca, Shourya Sarcar, Hilal Dib, Jeff Stanway, Frank Perbet, Nejc Trdin, Rachel Sterneck, Andrey Khorlin, Dinghua Li, Xihui Wu, Sonam Goenka, David Madras, Sasha Goldshtein, Willi Gierke, Tong Zhou, Yaxin Liu, Yannie Liang, Anais White, Yunjie Li, Shreya Singh, Sanaz Bahargam, Mark Epstein, Sujoy Basu, Li Lao, Adnan Ozturel, Carl Crous, Alex Zhai, Han Lu, Zora Tung, Neeraj Gaur, Alanna Walton, Lucas Dixon, Ming Zhang, Amir Globerson, Grant Uy, Andrew Bolt, Olivia Wiles, Milad Nasr, Ilia Shumailov, Marco Selvi, Francesco Piccinno, Ricardo Aguilar, Sara McCarthy, Misha Khalman, Mrinal Shukla, Vlado Galic, John Carpenter, Kevin Villela, Haibin Zhang, Harry Richardson, James Martens, Matko Bosnjak, Shreyas Rammohan Belle, Jeff Seibert, Mahmoud Alnahlawi, Brian McWilliams, Sankalp Singh, Annie Louis, Wen Ding, Dan Popovici, Lenin Simicich, Laura Knight, Pulkit Mehta, Nishesh Gupta, Chongyang Shi, Saaber Fatehi, Jovana Mitrovic, Alex Grills, Joseph Pagadora, Tsendsuren Munkhdalai, Dessie Petrova, Danielle Eisenbud, Zhishuai Zhang, Damion Yates, Bhavishya Mittal, Nilesh Tripuraneni, Yannis Assael, Thomas Brovelli, Prateek Jain, Mihajlo Velimirovic, Canfer Akbulut, Jiaqi Mu, Wolfgang Macherey, Ravin Kumar, Jun Xu, Haroon Qureshi, Gheorghe Comanici, Jeremy Wiesner, Zhitao Gong, Anton Ruddock, Matthias Bauer, Nick Felt, Anirudh GP, Anurag Arnab, Dustin Zelle, Jonas Rothfuss, Bill Rosgen, Ashish Shenoy, Bryan Seybold, Xinjian Li, Jayaram Mudigonda, Goker Erdogan, Jiawei Xia, Jiri Simsa, Andrea Michi, Yi Yao, Christopher Yew, Steven Kan, Isaac Caswell, Carey Radebaugh, Andre Elisseeff, Pedro Valenzuela, Kay McKinney, Kim Paterson, Albert Cui, Eri Latorre-Chimoto, Solomon Kim, William Zeng, Ken Durden, Priya Ponnapalli, Tiberiu Sosea, Christopher A. Choquette-Choo, James Manyika, Brona Robenek, Harsha Vashisht, Sebastien Pereira, Hoi

Lam, Marko Velic, Denese Owusu-Afriyie, Katherine Lee, Tolga Bolukbasi, Alicia Parrish, Shawn Lu, Jane Park, Balaji Venkatraman, Alice Talbert, Lambert Rosique, Yuchung Cheng, Andrei Sozanschi, Adam Paszke, Praveen Kumar, Jessica Austin, Lu Li, Khalid Salama, Bartek Perz, Wooyeol Kim, Nandita Dukkipati, Anthony Baryshnikov, Christos Kaplanis, XiangHai Sheng, Yuri Chervonyi, Caglar Unlu, Diego de Las Casas, Harry Askham, Kathryn Tunyasuvunakool, Felix Gimeno, Siim Poder, Chester Kwak, Matt Miecnikowski, Vahab Mirrokni, Alek Dimitriev, Aaron Parisi, Dangyi Liu, Tomy Tsai, Toby Shevlane, Christina Kouridi, Drew Garmon, Adrian Goedeckemeyer, Adam R. Brown, Anitha Vijayakumar, Ali Elqursh, Sadegh Jazayeri, Jin Huang, Sara Mc Carthy, Jay Hoover, Lucy Kim, Sandeep Kumar, Wei Chen, Courtney Biles, Garrett Bingham, Evan Rosen, Lisa Wang, Qijun Tan, David Engel, Francesco Pongetti, Dario de Cesare, Dongseong Hwang, Lily Yu, Jennifer Pullman, Srini Narayanan, Kyle Levin, Siddharth Gopal, Megan Li, Asaf Aharoni, Trieu Trinh, Jessica Lo, Norman Casagrande, Roopali Vij, Loic Matthey, Bramandia Ramadhana, Austin Matthews, CJ Carey, Matthew Johnson, Kremena Goranova, Rohin Shah, Shereen Ashraf, Kingshuk Dasgupta, Rasmus Larsen, Yicheng Wang, Manish Reddy Vuyyuru, Chong Jiang, Joana Ijazi, Kazuki Osawa, Celine Smith, Ramya Sree Boppana, Taylan Bilal, Yuma Koizumi, Ying Xu, Yasemin Altun, Nir Shabat, Ben Bariach, Alex Korchemniy, Kiam Choo, Olaf Ronneberger, Chimezie Iwuanyanwu, Shubin Zhao, David Soergel, Cho-Jui Hsieh, Irene Cai, Shariq Iqbal, Martin Sundermeyer, Zhe Chen, Elie Bursztein, Chaitanya Malaviya, Fadi Biadsy, Prakash Shroff, Inderjit Dhillon, Tejasi Latkar, Chris Dyer, Hannah Forbes, Massimo Nicosia, Vitaly Nikolaev, Somer Greene, Marin Georgiev, Pidong Wang, Nina Martin, Hanie Sedghi, John Zhang, Praseem Banzal, Doug Fritz, Vikram Rao, Xuezhi Wang, Jiageng Zhang, Viorica Patraucean, Dayou Du, Igor Mordatch, Ivan Jurin, Lewis Liu, Ayush Dubey, Abhi Mohan, Janek Nowakowski, Vlad-Doru Ion, Nan Wei, Reiko Tojo, Maria Abi Raad, Drew A. Hudson, Vaishakh Keshava, Shubham Agrawal, Kevin Ramirez, Zhichun Wu, Hoang Nguyen, Ji Liu, Madhavi Sewak, Bryce Petrini, DongHyun Choi, Ivan Philips, Ziyue Wang, Ioana Bica, Ankush Garg, Jarek Wilkiewicz, Priyanka Agrawal, Xiaowei Li, Danhao Guo, Emily Xue, Naseer Shaik, Andrew Leach, Sadh MNM Khan, Julia Wiesinger, Sammy Jerome, Abhishek Chakladar, Alek Wenjiao Wang, Tina Ornduff, Folake Abu, Alireza Ghaffarkhah, Marcus Wainwright, Mario Cortes, Frederick Liu, Joshua Maynez, Andreas Terzis, Pouya Samangouei, Riham Mansour, Tomasz Kępa, François-Xavier Aubet, Anton Algymr, Dan Banica, Agoston Weisz, Andras Orban, Alexandre Senges, Ewa Andrejczuk, Mark Geller, Niccolo Dal Santo, Valentin Anklin, Majd Al Merey, Martin Baeuml, Trevor Strohman, Junwen Bai, Slav Petrov, Yonghui Wu, Demis Hassabis, Koray Kavukcuoglu, Jeff Dean, and Oriol Vinyals. 2024a. Gemini 1.5: Unlocking multimodal understanding across millions of tokens of context. *Preprint*, arXiv:2403.05530.

Gemma Team, Thomas Mesnard, Cassidy Hardin, Robert Dadashi, Surya Bhupatiraju, Shreya Pathak, Laurent Sifre, Morgane Rivière, Mihir Sanjay Kale, Juliette Love, Pouya Tafti, Léonard Hussenot, Pier Giuseppe Sessa, Aakanksha Chowdhery, Adam Roberts, Aditya Barua, Alex Botev, Alex Castro-Ros, Ambrose Slone, Amélie Héliou, Andrea Tacchetti, Anna Bulanova, Antonia Paterson, Beth Tsai, Bobak Shahriari, Charline Le Lan, Christopher A. Choquette-Choo, Clément Crepy, Daniel Cer, Daphne Ippolito, David Reid, Elena Buchatskaya, Eric Ni, Eric Noland, Geng Yan, George Tucker, George-Christian Muraru, Grigory Rozhdestvenskiy, Henryk Michalewski, Ian Tenney, Ivan Grishchenko, Jacob Austin, James Keeling, Jane Labanowski, Jean-Baptiste Lespiau, Jeff Stanway, Jenny Brennan, Jeremy Chen, Johan Ferret, Justin Chiu, Justin Mao-Jones, Katherine Lee, Kathy Yu, Katie Millican, Lars Lowe Sjoesund, Lisa Lee, Lucas Dixon, Machel Reid, Maciej Mikuła, Mateo Wirth, Michael Sharman, Nikolai Chinaev, Nithum Thain, Olivier Bachem, Oscar Chang, Oscar Wahltinez, Paige Bailey, Paul Michel, Petko Yotov, Rahma Chaabouni, Ramona Comanescu, Reena Jana, Rohan Anil, Ross McIlroy, Ruibo Liu, Ryan Mullins, Samuel L Smith, Sebastian Borgeaud, Sertan Girgin, Sholto Douglas, Shree Pandya, Siamak Shakeri, Soham De, Ted Klimenko, Tom Hennigan, Vlad Feinberg, Wojciech Stokowiec, Yu hui Chen, Zafarali Ahmed, Zhitao Gong, Tris Warkentin, Ludovic Peran, Minh Giang, Clément Farabet, Oriol Vinyals, Jeff Dean, Koray Kavukcuoglu, Demis Hassabis, Zoubin Ghahramani, Douglas Eck, Joelle Barral, Fernando Pereira, Eli Collins, Armand Joulin, Noah Fiedel, Evan Senter, Alek Andreev, and Kathleen Kenealy. 2024b. Gemma: Open models based on gemini research and technology. *Preprint*, arXiv:2403.08295.

Hugo Touvron, Thibaut Lavril, Gautier Izacard, Xavier Martinet, Marie-Anne Lachaux, Timothée Lacroix, Baptiste Rozière, Naman Goyal, Eric Hambro, Faisal Azhar, Aurelien Rodriguez, Armand Joulin, Edouard Grave, and Guillaume Lample. 2023. Llama: Open and efficient foundation language models. *Preprint*, arXiv:2302.13971.

Qian Wang, Biao Zhang, Michael Birsak, and Peter Wonka. 2023. Instructedit: Improving automatic masks for diffusion-based image editing with user instructions. *Preprint*, arXiv:2305.18047.

Kai Zhang, Lingbo Mo, Wenhu Chen, Huan Sun, and Yu Su. 2024a. Magicbrush: A manually annotated dataset for instruction-guided image editing. *Preprint*, arXiv:2306.10012.

Shu Zhang, Xinyi Yang, Yihao Feng, Can Qin, Chia-Chih Chen, Ning Yu, Zeyuan Chen, Huan Wang, Silvio Savarese, Stefano Ermon, Caiming Xiong, and Ran Xu. 2024b. Hive: Harnessing human feedback for instructional visual editing. *Preprint*, arXiv:2303.09618.

Wanrong Zhu, Ruiyi Zhang, Jennifer Healey, William Yang Wang, and Tong Sun. 2024. Automatic layout planning for visually-rich documents with instruction-following models. In *Proceedings of the 3rd Workshop on Advances in Language and Vision Research (ALVR)*, pages 167–172, Bangkok, Thailand. Association for Computational Linguistics.

8 Appendix

We organize the appendix section into subsections to furnish additional details supporting our claims:

- Human Evaluation to derive the motivation of our research (Appendix 9)
- Related Works (Appendix 10)
- **SMARTEdit-Bench** Statistics
- **SMART-Editor** Methodology (Appendix 11)
  - Preprocessing Details of Images in **SMARTEdit-Bench** (Posters, Websites, Natural Images (Appendix 11.1)
  - Edit Instruction Taxonomy (Appendix 11.2)
  - Action Agent Details (Appendix 11.3)
  - Critique Agent Details (Appendix 11.4)
  - Optimizer Agent Details (Appendix 11.5)
- Implementation and Evaluation (Appendix 12)
  - Reference-Free Metrics (Appendix 12.1)
  - Reference-Based Evaluation Metrics on Structured Images (Appendix 12.2)
  - Reference-Based Evaluation Metrics on Un-Structured Images (Appendix 12.3)
  - Baseline Inference Prompting and Model Details (Appendix 12.5)
  - Composite Reward for Evaluation (Appendix 12.4)
  - DPO Implementation and Hyperparameters (Appendix 12.6)
- Additional Results on Automatic Evaluation (Appendix 13)
  - Reference-Based Evaluation on Websites and Posters (Table 12, Table 17), Reference-Free Evaluation on Websites (Table 18)
  - Impact of Training Data in DPO (Appendix 13.1)
  - Impact of Beam Search Iteration (Appendix 13.2)
  - Ablation of Reward Components in RewardRefine Approach (Appendix 13.3)
- Human Evaluation instructions and Consent Forms (Section 14)

9 Human Evaluation for Motivation

To assess whether the edit plans generated by VLMs and LLMs translate into coherent and reward-aligned edits, we conduct a human evaluation across 30 examples in each domain (Posters, Websites, Natural Images). For each sample, we provide human annotators (3 PhD students with design expertise) with the original image/layout, the model-generated plan, and the final layout/output after plan-to-command execution.

Annotators rate: (i) how well the plan aligns with the observed edit (Plan-to-Execution Match, 1–5), and (ii) the degree of overlap and alignment errors in the final layout (1–5, lower is worse). As shown in Table 7, posters show the highest alignment (avg. 4.45), with minimal overlap or misalignment. Websites perform slightly worse (4.18), while natural images show lower plan fidelity (3.70) and higher error scores, often due to weak grounding and spatial realism.

These results highlight a key gap in current models: while structured edits propagate well in posters and web layouts, plan-grounded editing in natural images is hindered by poor affordance reasoning and visual grounding. Importantly, failures identified by annotators—such as "misplaced added sections," "overlap with titles," or "semantic drift in relocated content"—correlate with quantitative penalties from our reward functions.

Setup. We selected 30 representative edit examples per domain (posters, websites, natural images). For each, we showed three expert annotators: (a) the input layout or image, (b) the edit instruction, (c) the plan generated by the VLM/LLM, and (d) the final output after applying the generated plan through command and execution steps.

Metrics. Annotators rated (1) how well the final output reflected the intended plan (Plan-to-Execution Match), and (2) the presence of overlap or misalignment based on visual inspection and design conventions (1–5 scale). Scores were averaged across annotators.

Participants. Three PhD-level design experts with prior experience in scientific poster creation and multimodal editing workflows.

Findings. Structured domains (posters, websites) exhibited strong plan adherence and minimal reward violations (Table 7). In contrast, image-based edits suffered from object overlap, layout incoherence, and inconsistencies between plan and outcome, reflecting weak model grounding in unstructured visual tasks.

Domain	Plan-to-Execution Match (1–5)	Avg. Overlap Violation	Avg. Alignment Error
Posters	4.45 ± 0.31	1.22 ± 0.45	1.40 ± 0.51
Websites	4.18 ± 0.39	1.50 ± 0.62	1.68 ± 0.58
Natural Images	3.70 ± 0.55	2.10 ± 0.70	1.90 ± 0.65

Table 7: Human evaluation of plan-to-execution consistency and reward function failures (rated 1–5) across 30 samples per domain by 3 expert annotators. Lower scores indicate more frequent violations.

10 Related Work

Our work intersects multiple areas of research, including instruction-based image editing, layout and structure-preserving generation, and cascading edit reasoning. We organize the discussion into four main categories: **(1) Instruction-Based Image Editing**, **(2) Structured Layout Editing**, **(3) Compositional and Cascading Reasoning**, and **(4) Programmatic and Code-Based Edit Modeling**.

Instruction-Based Image Editing. Instruction-guided image editing has emerged as a key task to enable intuitive human-AI interaction. Early models such as **InstructPix2Pix** (Brooks et al., 2023) pioneered fine-tuning diffusion models using instruction–image pairs generated by LLMs. However, their reliance on synthetic data often introduced hallucinations or poor alignment. Recent datasets aim to address these limitations. **HumanEdit** (Bai et al., 2025) introduces a high-quality, human-rewarded dataset of over 5,000 examples with edit masks and naturalistic instructions across six fine-grained types (e.g., 'Add a butterfly," 'Reduce grapes from 3 to 2"). **HQ-Edit** (Hui et al., 2024) scales up this vision by synthetically generating 200,000 edit pairs using GPT-4V and DALLE 3 with enhanced instruction diversity and layout coherence via post-processing. It introduces alignment and coherence metrics to assess semantic fidelity. However, both focus on **visual realism and localized edits**, without modeling or evaluating how edits should propagate structurally across interdependent layout elements. Other image-editing systems, such as **MagicBrush** (Zhang et al., 2024a), HIVE (Zhang et al., 2024b) and **SEED-Data-Edit** (Ge et al., 2024), fine-tune LDMs for instruction-following using structured or crowd-annotated masks. While these methods improve local edit adherence, they do not address whether **cascading implications** of edits are correctly realized in a structured scene or layout.

Structured Layout Generation Structured layout generation has gained attention for tasks such as UI prototyping, poster generation, and scientific visualization. Models like **LayoutGAN** (Li et al., 2019), **LayoutVAE** (Jyothi et al., 2021), and **LayoutTransformer** (Chai et al., 2023) learned to place elements based on supervised geometric and semantic patterns.

With the rise of LLMs, **LayoutGPT** (Feng et al., 2023b) proposed using LLMs to serve as visual planners by converting textual instructions into HTML-style structured layouts. Similarly, **LayoutCoT** (Shi et al., 2025) demonstrates that CoT reasoning and retrieval-augmented generation can help LLMs improve alignment and visual coherence in layout generation. However, both target layout *synthesis*, not **iterative layout editing**, and lack evaluation mechanisms for edit propagation. **SciPostLayout** (Tanaka et al., 2024) introduces a dataset of scientific poster layouts, enabling research into layout understanding. Yet it focuses on static layout prediction and lacks instructional editing or reasoning evaluation. **InstructEdit** (Wang et al., 2023) explores using instructions to guide edits, optimizing for downstream engagement (social media) or using segmentation for precise control. These approaches are instructive for our work but again, they operate at the **pixel-level or object-level**, not layout-structure.

Compositional and Cascading Reasoning in Layouts Humans perform layout edits not just locally, but with global awareness—adding a new section may require shifting others, updating order, and maintaining alignment. Existing editing benchmarks (e.g., **GraphicBench**) focus on agent planning and multimodal synthesis but do not evaluate how edits *cascade* through a layout. To this end, we introduce **SMARTEditBench**, a benchmark for testing whether multimodal LLMs can handle *compositional reasoning* in edits—e.g., does repositioning one figure preserve alignment with its caption? Can adding a section reorder surrounding elements semantically? Our method evaluates edits in structured settings like posters, web layouts, and scenes using metrics like **semantic ordering, spa-**

tial overlap, and visual alignment. This direction is loosely inspired by structured editing tasks in other modalities, such as **semantic parsing** with structured outputs, but uniquely adapted for **visual-semantic alignment and layout reasoning**.

Programmatic Editing and Code-Driven Reasoning. Recent research investigates editing behaviors over code or structured representations. Instruction-following models for **code editing** (e.g., CodeX (Chen et al., 2021), InCoder (Fried et al., 2023)) have demonstrated impressive reasoning about insertion, deletion, and reordering in code. In a similar vein, some web-editing models like **EditNet** (Li et al., 2022) predict edit actions over HTML based on goal descriptions. In the vision domain, LayoutGPT (Feng et al., 2023b) uses a stylesheet-style intermediate representation to enable compositional planning. Our work draws on these insights and applies them to layout editing, where bounding box structures and section types must be jointly updated to follow instructions while preserving document integrity. In contrast to prior work focused on localized edits, synthetic instruction adherence, or single-step generation, our framework evaluates whether multimodal models can perform **cascading, multi-element, instruction-based layout refinement**. We propose a new benchmark (*SMARTEditBench*), and evaluation protocols to test whether edits to one element propagate logically and semantically across a structured scene or document.

11 SMART-Editor Methodology

11.1 Preprocessing Details

To enable structured layout reasoning across diverse input formats, we apply modality-specific preprocessing techniques to convert unstructured inputs into a unified representation: a set of objects or sections, each with a bounding box and textual content. Below we describe the processing pipeline for each modality: To enable structured layout reasoning across diverse input formats, we adopt modality-specific preprocessing pipelines that convert raw visual or web-based inputs into a unified representation consisting of objects or sections with associated bounding boxes and textual content.

For **natural images**, we begin with a raw image and a textual edit instruction (e.g., "Add a cat on the left"). We use `spaCy` to extract noun phrases from the instruction, which are then treated as grounding targets for **Grounding DINO** (Ren et al., 2024). The detected regions are further refined using the **Segment Anything Model (SAM)** (Kirillov et al., 2023), which improves the quality of object-level masks and bounding boxes. This process yields a set of annotated objects with precise spatial regions and semantic labels.

For **scientific posters**, we leverage GPT-4o to extract structured layout elements directly from poster screenshots or PDF renderings. We prompt the model with a query such as: *"Given this poster, identify all distinct rectangular sections and provide their bounding boxes and associated content in the format {section name: [x1, y1, x2, y2], content: "..." }"*. GPT-4o returns a structured layout with section-wise bounding boxes and corresponding textual descriptions, enabling layout-aware downstream reasoning.

For **websites**, we parse HTML DOM tree using tools such as `BeautifulSoup` or `lxml` to extract key structural components, including headers, navigation bars, content blocks, and sidebars. We retrieve the text content for each major DOM node and estimate their bounding boxes using browser-based rendering APIs (e.g., via `Playwright` or headless browser utilities). The result is a structured mapping from each layout region to its geometric footprint and textual content, making it compatible with layout editing models.

11.2 Edit Instruction Taxonomy

Table 9 provides illustrative examples of edit instructions spanning diverse modalities (posters, websites, and natural images), each annotated with a corresponding taxonomy of edit type, degree of explicitness, and need for cascaded changes. We distinguish between five types of structural edits: **Section Reordering**, **Section Insertion**, **Object Replacement**, **Content Grouping**, and **Section Deletion**. These edit types are frequently encountered across structured and unstructured domains in our benchmark. An important dimension captured in this table is **implicitness**—i.e., how much of the required layout or content adjustment is left unstated in the instruction. For instance, even simple insertions (e.g., adding a section) demand implicit reasoning about placement and formatting, while object replacement in natural images often assumes background compatibility and spatial realism. We also highlight whether edits cause **cas-**

Domain	#Edits	Source	Annotations
Webpages (Real)	564	GitHub + GPT-4V	Edit Type + Reasoning (Gold Edited Output)
Webpages (Synthetic)	510	Design2Code + GPT-4o	Edit Type + Reasoning (Gold Edited Output)
Posters (Synthetic)	1,200	SciPostLayout + GPT-4o	Edit Type + Reasoning (No Gold Edited Output)
Posters (Human Eval)	250	Expert-Tagged Posters	Gold Edited Output
Natural Images	—	HQ-Edit (Scene Edits)	Object-Level Semantics (Gold Edited Output)

Table 8: Composition of SMARTEditBench across modalities and sources.

Edit Instruction	Taxonomy	Modality	How is it Implicit?	Cascaded Change?
Move the "Results" section above "Methods"	Section Reordering	Poster	Requires understanding of scientific discourse order (Results should follow Methods)	Yes
Add a section describing ongoing research projects below the About section	Section Insertion	Website	Implies structural addition and reflowing of layout without stating exact position or formatting	Yes
Replace the "silver teapot" with a "sleeping tabby cat" in the image	Object Replacement	Natural Image	Requires inferring spatial placement (e.g., "on table"), relative size, and plausibility	Yes
Group all job experiences by company to make the layout more readable	Content Grouping	Website	Suggests structural reorganization without detailing how the layout should shift	Yes
Remove the References section	Section Deletion	Poster	Directly states which section to delete, but doesn't specify consequences on layout alignment or spacing	Yes

Table 9: Examples of edit instructions with associated taxonomy, modality, nature of implicit reasoning, and whether the edit requires cascaded changes.

caded changes—that is, whether making the instructed change necessitates updates to surrounding layout structure, alignment, or spacing. Most implicit instructions lead to cascaded layout effects, making them particularly challenging for models that rely on direct decoding without structural reasoning. This taxonomy informs our design of evaluation settings and is central to motivating the need for structured, multi-step editing pipelines like SMART-Editor.

11.3 Action Agent Details

The action agents takes in the layout and content extracted from an image, translates the implicitly specified edit instruction in the layout-content space into verbal action plan, next the actions are transformed into specific modular functions (Description of modular functions in 10 and the implementation of each of these functions are in ALgorithm 3, ALgorithm 4, ALgorithm 5 and ALgorithm 6) which when executed should lead to the refined layout-content output.

Prompt: Action Plan Generation

You are provided with a structured layout consisting of bounding boxes and their associated section labels, along with an edit instruction that specifies how the layout should be changed.

Your task is to generate a clear and concise step-by-step **action plan in natural language** that explains:

- Which specific sections need to be added, removed, or modified.
- What geometric adjustments are required, such as moving, resizing, or swapping sections.
- The reasoning behind these changes, ensuring that layout coherence is preserved—for example, avoiding overlaps or maintaining narrative flow.

Edit Instruction:
`{edit_instruction}`

Initial Layout:
`{initial_layout}`

(Each entry includes a section ID, bounding box coordinates $[x_0, y_0, x_1, y_1]$, and a section label.)

Expected Output:
Write a natural language action plan describing the semantic and spatial edits needed to fulfill the instruction. Avoid code or structured formats—this should be a verbal plan intended for a layout editing agent to interpret and execute.

Target Action Driven Action-Plan

You will be provided with an action plan corresponding to an edit instruction `{edit_instruction}` and a set of target geometric actions. Your job is to convert the plan into steps of geometric actions that would be integrated into the code sequentially.

Action Plan (in words)
`{Action_plan}`

Geometric Action Codes
`{geometric_actions}`

Initial Layout
`{initial_layout}`

Output Format
Format your output as a list of JSON objects containing the sequence of target action APIs by filling in the real values of parameters inside the functions. Do not output anything else.
The output should match the exact format in the Geometric Action Codes, for example:
`snap_to_grid(layout: Layout, section_id: str, grid_unit)`
`resize_section(layout: Layout, section_id, scale_x, scale_y)`
Each output JSON object must contain two keys: `action` and `parameters`.

11.4 Critique Agent Details

11.4.1 Critiques for Unstructured Images

To evaluate image edits in unstructured domains (e.g., natural images), we introduce a suite of **critique agents** that analyze various dimensions of visual quality, semantic fidelity, and instruction alignment. These agents leverage both automated metrics and LLM-based reasoning to generate fine-grained, actionable feedback. These agents are based on the way it is specified in Appendix 12.3. Each critique agent is assigned to evaluate one axis of visual quality:

- **Edit Adherence (EA)**: Determines whether the edited image faithfully executes the textual instruction. Agents examine both the visual edit and the original instruction to rate adherence on a scale from 1 (failed to follow) to 5 (precise execution).
- **Semantic Match (CLIP Similarity)**: Uses CLIP-based cosine similarity to assess alignment between the instruction and the resulting image. Agents consider object presence, type, and contextual placement.
- **Object Realism**: Judges whether objects appear naturally scaled and spatially integrated within the scene. Edits that result in unrealistic overlaps, floatation, or unnatural proportions receive lower scores.
- **Depth and Occlusion**: Evaluates the spatial layering of objects. If any object appears visually inconsistent (e.g., floating, occluded unnaturally), the agent marks the edit as implausible.

Critique Prompting Protocol For each edited image, we gather the following:

- Instruction used for editing
- Edited image (visual or VLM-encoded)
- Per-dimension scores (1–5 scale or cosine similarity)

The critique agent is prompted as follows:

> `You are a critique agent. The instruction was: "Add a coffee cup on the table." You are provided with:`
>
> - `Edited Image: [image or feature representation]`
> - `Adherence Score: 4`
> - `Semantic Match (CLIP): 0.72`
> - `Object Realism Score: 3`
> - `Depth/Occlusion Score: 2`
>
> `For each dimension, describe (a) what went well, (b) what went wrong, and (c) one specific suggestion to improve the edit. Output a structured critique across all dimensions.`

The agent returns feedback in a structured JSON format, identifying strengths and weaknesses in each dimension. This feedback is used to guide model refinement or generate revision plans in downstream modules.

Composite Reward and Feedback Trace. The composite reward for an unstructured image is computed by summing the individual dimension scores. Critique agents trace the reward breakdown to pinpoint low-performing aspects, providing a transparent rationale for model evaluation and improvement.

Function	Description	Example	LaTeX Symbolic Form
`translate_object`	Shifts a section's position by Δx, Δy.	Translate `METHODS` by $(0, +100)$	$\text{bbox}' = \text{bbox} + (\Delta x, \Delta y)$
`resize_object`	Scales the width and height of a section by s_x, s_y.	Resize `PLOT 1` by $(s_x = 1.2, s_y = 0.8)$	$\text{bbox}' = \text{scale}(\text{bbox}, s_x, s_y)$
`align_object_left`	Aligns the left edge of a section to a reference x.	Align `BACKGROUND` to $x = 30$	$x_1' = x_{\text{ref}},\ x_2' = x_{\text{ref}} + w$
`center_object`	Centers the section horizontally within canvas width W.	Center `ACKNOWLEDGEMENTS` on canvas of width 1080	$x_1' = \frac{W-w}{2},\ x_2' = x_1' + w$
`snap_to_grid`	Snaps bbox edges to nearest grid unit δ.	Snap `REFERENCES` to grid of 20px	$x_i' = \delta \cdot \lfloor \frac{x_i}{\delta} + 0.5 \rfloor$
`insert_object`	Inserts a new section with given bbox and text.	Insert `SUMMARY` at $[100, 500, 400, 580]$	$\text{layout}[s] = \{\text{bbox}, \text{text}\}$
`remove_object`	Deletes a section from layout by ID.	Remove `INTRODUCTION`	$\text{layout} = \text{layout} \setminus \{s\}$
`replace_object_bbox`	Replaces the bbox of a section with a new one.	Replace `METHODS` bbox to $[50, 400, 480, 500]$	$\text{layout}[s].\text{bbox} \leftarrow \text{new_bbox}$
`reorder_objects`	Reorders sections top-down with optional spacing.	Reorder [`INTRO`, `METHOD`, `RESULT`] with $y_{\text{pad}} = 20$	$y_i' = y_0 + \sum_{j=1}^{i-1}(h_j + y_{\text{pad}})$
`update_object_text`	Updates the text content of a section.	Update `RESULT` text to "New findings here."	$\text{layout}[s].\text{text} \leftarrow \text{new_text}$

Table 10: Layout editing functions with their semantic descriptions, practical examples, and symbolic representations. All the implementation algorithms are listed in Algorithm 1-4.

11.4.2 Critiques for Structured Image Edits

To evaluate structured document layouts such as posters and websites, we design critique agents that assess both spatial and semantic alignment of layout edits with the instructional goal. Each agent receives the edit trace (instruction, initial layout, final layout), computed reward scores, and generates targeted, actionable feedback.

Critique Dimensions Each critique agent is responsible for one of the following layout quality metrics as calculated in Appendix 12.1. Each agent is provided with the following:

- **Edit Instruction**: Natural language instruction (e.g., "Move Results above Methods")
- **Layout JSONs**: Initial and edited layouts with bounding boxes and content
- **Reward Values**: Pre-computed scores from layout evaluators (e.g., overlap, alignment)

Each critique agent is prompted as:

> For each dimension, write: 1. What is good or bad 2. What causes the issue 3. How to revise the layout to improve it

Agents return structured rationales (e.g., in JSON or Markdown) identifying violations and suggesting layout edits such as repositioning, snapping to grid, or restructuring slide order. These are used downstream by the Optimizer Agent to

11.5 Optimizer Agent Details

12 Implementation and Evaluation Details

12.1 Reference-Free Evaluation

In Table 2 and Table 18, we have used the following reference-free metrics/rewards to calculate which do not assume any gold-standard image to compare.

1. Edit Adherence (EA) Evaluation

You are given a layout editing task. Based on the **Edit Instruction**, the system updates the layout and content. You are asked to rate how faithfully the instruction was followed.
Edit Instruction: `<Insert instruction here>`

Initial Layout and Content:
`<Insert JSON-like structure for layout and section content before edit>`

Final Layout and Content:
`<Insert JSON-like structure for layout and section content after edit>`

Question: On a scale from 1 to 5, how well does the final layout implement the edit instruction?

1: Edit is incorrect or missing.

3: Edit partially follows the instruction.

5: Edit fully implements the instruction as intended.

Your Response:
Score (1–5): _____ Justification:
[redacted]

Narrative Coherence (Narr.) Evaluation. To evaluate the **Narrative Coherence (Narr.)** (r_{sem}) evaluates whether the edited layout preserves the top-down logical structure of a document (e.g., *Background* $\rightarrow$ *Methods* $\rightarrow$ *Results*). For each pair of expected section orders (S_i, S_j), GPT-4o is prompted with: *"Does section S_i logically precede section S_j?"*. A violation is counted if the answer is negative. The final reward is computed as

$$r_{\text{sem}} = 1 - \frac{v}{|\mathcal{O}|}$$

where v is the number of violations and $\mathcal{O}$ is the set of all ordered section pairs. This reward ensures that edits do not disrupt the logical reading flow of the content (Refer to Examples in Table 11).

Cross-Sectional Consistency Evaluation. (r_{cross}) measures whether semantically linked content—such as figures and their captions or methods and results—remain meaningfully consistent. GPT-4o is treated as a natural language inference model, where each section pair (S_i, S_j) is evaluated for entailment. If GPT-4o detects a semantic contradiction, it is counted as a violation. The reward is defined as

$$r_{\text{cross}} = 1 - \frac{c}{|\mathcal{G}|}$$

where c is the number of contradictions and $\mathcal{G}$ is the set of grouped section pairs. This metric ensures semantic alignment across logically related content blocks (Refer to Examples in Table 11).

Overlap Penalty (Ovlp). It quantifies undesirable visual collisions between elements. For every pair of layout components $(\mathbf{b}_i, \mathbf{b}_j)$, the intersection-over-union (IoU) is computed if they overlap, and accumulated as a penalty. This discourages any spatial overlap that could hinder readability or visual clarity.

Whitespace Penalty (Wspc). It inefficient use of layout space. It is defined as

$$1 - \frac{A_{\text{used}}}{A_{\text{canvas}}}$$

where A_{used} is the total area of layout boxes and A_{canvas} is the total canvas area. This encourages layouts to use space compactly, without excessive gaps that reduce visual coherence.

Alignment Reward (Algn). It encourages the visually aligned layouts by rewarding sections whose left edges fall on predefined grid lines. Let x_i be the left edge of bounding box $\mathbf{b}_i$. Then, the alignment reward is computed as

$$r_{\text{align}} = \frac{1}{N} \sum_{i=1}^{N} I[x_i \bmod \text{grid} = 0]$$

where N is the total number of layout components. This promotes clean and structured alignment across the layout.

12.2 Reference-Based Evaluation Prompts on Structured Domains

In this section, we discuss about the different evaluation metrics that we use to compare the model-edited images with the human-edited images (gold-standard) on the structured domains of images such as posters and websites **SMARTEdit-Bench**-Posters and **SMARTEdit-Bench**-Websites respectively. To evaluate, we use the following prompts using GPT4-o as Judge as mentioned below, and the results are tabulated in Table 12 and Table 17.

Semantic Consistency (Reference-Based)

Compare the model-edited layout and content with a human-edited (gold) version.
Instruction: "Move Results above Methods"

Metric	Description (GPT-4o-Inferred)
Narrative Coherence	Assesses whether the document follows a top-down logical structure (e.g., Background → Methods → Results). For each section pair (S_i, S_j) in the expected order, GPT-4o is prompted with: "Does the content of section 'S_i' logically precede section 'S_j'?". If GPT-4o responds "no," the pair is marked as a violation. The final reward is computed as $r_{\text{sem}} = 1 - \frac{v}{\lvert\mathcal{O}\rvert}$, where v is the number of violations and $\mathcal{O}$ is the set of expected pairs.
Cross-Sectional Consistency	Measures semantic contradictions across grouped section pairs (e.g., Figure and its Caption, or Methods and Results). GPT-4o is used as an NLI model: section S_i serves as the premise, S_j as the hypothesis. It is prompted to determine whether the pair is entailed, neutral, or contradictory. If the label is "contradiction," it is counted as a violation. The reward is defined as $r_{\text{cross}} = 1 - \frac{c}{\lvert\mathcal{G}\rvert}$, where c is the number of contradictions and $\mathcal{G}$ is the set of grouped section pairs.

Table 11: Description of semantic reward metrics inferred using GPT-4o.

Model Output: ...
Gold Output: ...
Task: Rate semantic consistency on a scale from 1 (completely misaligned) to 5 (semantically faithful to the gold).

Layout Similarity (Reference-Based)

Compare the spatial arrangement and section order of the model-edited layout to the gold layout.
Ignore text content; focus only on structural similarity.
Model Layout: ...
Gold Layout: ...
Rate similarity from 1 (very different) to 5 (nearly identical).

12.3 Reference Based Evaluation on Unstructured Images

In this section, we discuss about the different evaluation metrics that we use to compare the model-edited images with the human-edited images (gold-standard) on the natural images in **SMARTEdit-Bench**-Natural Images. To evaluate, we use the following prompts using GPT4-o as Judge as mentioned below, and the results are in Table 3.

Image Edit Adherence

Given an image edit instruction and a generated image, assess whether the instruction was accurately followed.
Instruction: "Replace the tiger with a small cat on the right side."
Edited Image: [VLM View or Image ID]
Reference (Gold): [Reference Image or CLIP Caption]
Rate from 1 (failed to follow) to 5 (precise and faithful execution).

Semantic Match (CLIP Similarity)

Compute the CLIP similarity between the textual instruction and the generated image. Use this to judge whether the object(s), their type, and placement are semantically aligned with the intent.
Instruction: "Add a dog sitting under a tree"
Image: [CLIP-encoded]
Score: cosine similarity between instruction and image features.

Object Size and Overlap Realism

Check if the edited image contains objects that appear too large, too small, or overlap unnaturally.
Instruction: "Add a coffee cup on the table"
Image: [generated]
Rate from 1 (poor realism) to 5 (realistic object size and spatial integration).

Depth and Occlusion (Unstructured)

Evaluate whether the spatial layering of objects appears natural. Are any objects unnaturally floating, occluded, or visually inconsistent?
Edited Image: [image]
Rate from 1 (unrealistic occlusion or depth) to 5 (physically plausible arrangement).

12.4 Composite Reward Calculation for Structured and Unstructured Images

In the case of natural images (unstructured), the **Composite Reward** used in Figure 4 evaluates whether the edited image aligns with user intent and preserves visual realism. It combines all the rewards mentioned in Section 12.3. The VLM generated scores are in the range of 1-5. These are summed to yield the final score which ensures that image edits remain semantically faithful, physically grounded, and visually plausible. And in the case of posters and websites (structured), the **Composite Reward** used in Figure 4 combines all the rewards and penalties mentioned in Section 12.1.

12.5 Baseline Inference Prompting and Model Details

Zero-Shot Prompt: Layout Inference

You are a layout editing assistant. Your task is to update the structure of a poster or webpage layout in response to a human instruction. **Instruction:** `Move the Results section above Methods`
Initial Layout: `{Initial_layout}`
Initial Content: `{Initial_Content}`
Output: Return the updated layout as a JSON dictionary. Do not explain your answer.

Chain-of-Thought Prompt: Step-by-Step Layout Reasoning

You are a layout editor that follows human design principles. Think step-by-step to apply the edit instruction to the layout.
Instruction: `Insert a new section titled Discussion below Results`
Initial Layout: `{Initial_layout}`
Step-by-Step: 1. The instruction asks to insert "Discussion" below "Results".
2. "Results" ends at y=500.
3. Allocate a height of 100 for the new section.
4. Add new bounding box for "Discussion": `[0, 500, 768, 600]`
Updated Layout: `{Updated_layout}`

Few-Shot Prompt: Layout Editing with Examples

You are a layout editing assistant. Your task is to revise the layout structure based on edit instructions, layout geometry, and section content.
— Example 1 —

— Example 2 —

— Now You Try —
Instruction: `Swap Methods and Study Participants`
Initial Layout: `{Initial_layout}`
Initial Content: `{Initial_Content}`
Output: Provide updated layout only.

Inference Settings We evaluate the performance of LLMs and VLMs on layout and content editing using a consistent set of inference-time hyperparameters. Table summarizes the decoding configurations used for each model. For HuggingFace-hosted models such as Gemma (gemma-2-9b-it) ([2]), LLama (Llama-3.2-3B-Instruct),[3] Qwen[4]), LLaVA (LLava-1.5-7b,[5] we follow standard generation protocols. For GPT-4o and Gemini-Pro, we rely on their respective APIs.

Default Generation Configuration. Unless otherwise specified, models are run with the following decoding settings:

- `max_new_tokens = 1024`
- `temperature = 0.7`
- `top_p = 0.9`, `top_k = 50`
- `repetition_penalty = 1.1`
- `do_sample = True`, `num_beams = 1`

Special Use Cases. For REWARD-REFINE, we enable `num_beams = 5` to allow multi-candidate sampling. For VLMs such as LLaVA or GPT-4o, structured visual layouts are encoded as textual descriptions of bounding boxes and section names when images are not directly available.

[2] https://huggingface.co/google/gemma-2-9b-it
[3] https://huggingface.co/meta-llama/Llama-3.2-3B-Instruct
[4] https://huggingface.co/Qwen/Qwen2.5-7B-Instruct
[5] https://huggingface.co/liuhaotian/llava-v1.5-7b

Model	Avg. SC (1–5) ↑	Avg. LS (1–5) ↑
LayoutPrompter (Lin et al., 2023)	-	4.01 (±0.00)
LLaMA (Zero-Shot)	4.14	3.90 (-0.11)
LLaMA + Reward-Refine	4.00	4.05 (+0.04)
LLaMA + RewardDPO	4.12	4.18 (+0.17)
Gemma (Zero-Shot)	4.10	3.78 (-0.23)
Gemma + Reward-Refine	3.88	3.93 (-0.08)
Gemma + RewardDPO	4.01	4.10 (+0.09)
Qwen (Zero-Shot)	3.11	3.97 (-0.04)
Qwen + Reward-Refine	3.88	4.03 (+0.02)
Qwen + RewardDPO	4.01	4.10 (+0.09)
LLaVA (Zero-Shot)	4.00	3.55 (-0.46)
LLaVA + Reward-Refine	3.75	3.72 (-0.29)
Gemini-Pro (Zero-Shot)	4.00	3.78 (-0.23)
Gemini-Pro + Reward-Refine	4.30	4.38 (+0.37)
GPT-4o (Zero-Shot)	4.52	3.98 (-0.03)
GPT-4o + Reward-Refine	**4.38**	**4.47 (+0.46)**

Table 12: Reference-based Evaluation on the **SMARTEditBench-Posters**, comparing **Zero-Shot**, **Reward-Refine**, and **RewardDPO** variants against the current state-of-the-art training-free model, **LayoutPrompter**, using human-edited posters as the gold standard. We report average GPT-4o scores (on a 1–5 scale) for two dimensions: *Semantic Consistency (SC)* and *Layout Similarity (LS)*. Delta values denote the improvement over the baseline LayoutPrompter (SC score of 4.01), where higher positive deltas reflect better alignment with human-edited layouts.

12.6 DPO Implementation and Hyperparameters

For DPO training, we fine-tuned both `LLaMA-3-8B-Instruct` and `Gemma-2-9B-It` using full-parameter tuning across all layers. We employed a sigmoid-based preference loss with $\beta = 0.1$, a learning rate of 5×10^{-7} with cosine decay, and a warmup over 10% of total steps. Training was run for 3 epochs with a batch size of 1 and gradient accumulation steps of 8. We used `bfloat16` precision and optimized training efficiency with DeepSpeed ZeRO Stage 3. Model evaluation was performed every 100 steps, and logs were recorded every 10 steps to monitor convergence behavior. Training was conducted on 4 A100 80GB GPUs and took approximately 5 GPU-hours per model. The total compute budget, including data preprocessing and reward-based filtering, was approximately 20 GPU-hours.

13 Additional Results on Automatic Evaluation

13.1 Impact of Training Data in DPO

To assess how much preference data is required for effective reward-based fine-tuning, we conduct an ablation study varying the number of training pairs used in RewardDPO across posters, websites, and natural images. As shown in Table 14, performance improves steadily as training data increases from 1.2k (10%) to 4k (30–35%), but plateaus beyond that. Notably, models trained with just 4k preference pairs achieve near-saturation in all domains, yielding 97–99% of the gains observed with the full 12k set. For structured domains like posters and websites, edit adherence (EA), semantic consistency (SC), and layout similarity (LS) scores reach above 4.3 by this point. Similarly, in natural images, key realism dimensions such as depth layering (DL), semantic match (SM), and overlap plausibility also converge early, with only marginal improvements (+0.02 to +0.05) when scaling to 12k pairs.

These results suggest that RewardDPO requires relatively modest supervision to internalize layout-sensitive preferences. Efficient learning is likely due to the structured nature of the reward signals and the contrastive framing of the optimization objective. This finding supports the scalability of preference-based finetuning in layout editing tasks—even in low-resource or domain-adaptive settings.

13.2 Beam Search Ablation

We ablate the impact of beam width on layout edit quality across structured and unstructured domains. As shown in Table 15, increasing the beam size from 1 (greedy) to 4 leads to consistent improve-

Training Size (Pairs)	Posters (EA / SC / LS)	Websites (EA / SC / LS)	Images (EA / DL / SM / Overlap)
10% (1.2k)	4.12 / 4.00 / 4.08	4.08 / 3.92 / 4.01	4.10 / 4.00 / 4.10 / 4.00
30% (4k)	**4.32 / 4.25 / 4.30**	**4.26 / 4.18 / 4.22**	**4.32 / 4.20 / 4.35 / 4.22**
100% (12k)	4.35 / 4.32 / 4.35	4.30 / 4.25 / 4.30	4.35 / 4.20 / 4.40 / 4.25

Table 14: Ablation on RewardDPO training data volume across domains. Performance converges around 4k preference pairs, with only marginal gains beyond. EA: Edit Adherence, SC: Semantic Consistency, LS: Layout Similarity, DL: Depth Layering, SM: Semantic Match.

Beam Width	Posters (EA / SC / LS)	Websites (EA / SC / LS)	Images (EA / DL / SM / Overlap)
1 (Greedy)	4.10 / 3.95 / 4.05	4.02 / 3.88 / 3.95	4.05 / 3.90 / 4.00 / 3.88
2	4.20 / 4.10 / 4.18	4.15 / 4.00 / 4.08	4.15 / 4.00 / 4.12 / 4.00
4	**4.32 / 4.25 / 4.30**	**4.26 / 4.18 / 4.22**	**4.32 / 4.20 / 4.35 / 4.22**
6	4.33 / 4.26 / 4.31	4.28 / 4.19 / 4.23	4.33 / 4.20 / 4.35 / 4.23
8	4.33 / 4.25 / 4.30	4.28 / 4.18 / 4.23	4.32 / 4.20 / 4.34 / 4.22

Table 15: Beam search ablation across domains. Performance improves notably from greedy decoding to beam size 4, with diminishing returns beyond. EA: Edit Adherence, SC: Semantic Consistency, LS: Layout Similarity, DL: Depth Layering, SM: Semantic Match.

ments across all metrics, including Edit Adherence (EA), Semantic Consistency (SC), and Layout Similarity (LS). For example, in posters, performance improves from 4.05 (LS) under greedy decoding to 4.30 at beam size 4. Similarly, in natural images, realism dimensions such as Depth Layering (DL) and Semantic Match (SM) also improve.

Beyond a beam width of 4, gains plateau across domains, indicating early convergence. Beam sizes larger than 6 offer minimal additional benefit while increasing computational cost. These results suggest that beam width 4 offers a strong trade-off between performance and efficiency in layout-aware decoding.

13.3 Impact of Reward Components in RefineLoop

To assess which reward signals are most critical for aligning model edits with gold references, we ablate individual components within RefineLoop and evaluate the resulting outputs using GPT-4o-based reference comparison. As shown in Table 16, removing *alignment* or *semantic order* results in the largest quality drops in structured domains, reflecting their importance in enforcing visual structure and narrative flow. In contrast, for natural images, removing *overlap realism* sharply degrades plausibility, reducing the score from 4.25 to 3.90. Spatial-only rewards (alignment + overlap) perform well on images, while semantic-only rewards (semantic order + cross-sectional consistency) fall short in layout tasks. These findings validate the role of targeted reward components in generating edits that align with human design expectations.

14 Human Evaluation

The instructions provided to the humans for performing annotations are illustrated in Figure 12 and the form to collect their consent is in Figure 13.

Algorithm 1 Reward-Guided Layout and Content Refinement

Input: Layout data D (e.g., webpage, PDF, or image), instruction I
Output: Final layout L^* and content C^*
Step 1: Layout Representation
Convert D into unified layout $L_0 = \{(o_i, \mathbf{b}_i, t_i)\}_{i=1}^N$ and initial content C_0
Step 2: Instruction Classification
Classify instruction I as `layout-only`, `semantic-only`, or `joint-edit`
Step 3: First-Pass Execution
Generate symbolic action plan $A = [a_1, \ldots, a_k]$ using an LLM
Apply actions to obtain layout L' and updated content C':

$$L', C' \leftarrow a_k(\ldots a_1(L_0, C_0))$$

Step 4: Reward Evaluation
Compute layout reward: $R(L') = \sum_k \lambda_k \cdot r_k(L')$
if $R(L') < \tau$ or constraints are violated **then**
    Initialize $L^{(0)} \leftarrow L'$, $C^{(0)} \leftarrow C'$
    for $t = 1$ to T **do**
        Generate k layout-content candidates via beam search on $(L^{(t-1)}, C^{(t-1)}, I)$
        Select best candidate: $(L^{(t)}, C^{(t)}) \leftarrow \arg\max R(L)$
        if $L^{(t)}$ satisfies all constraints **then**
            return $L^* = L^{(t)}, C^* = C^{(t)}$
        end if
        Generate feedback f_t (e.g., "Results overlaps with Discussion")
        Refine via LLM: $(L^{(t)}, C^{(t)}) \leftarrow$ `LLM_Refine`$(L^{(t)}, C^{(t)}, I, f_t)$
    end for
end if
return $L^* = L'$ or $L^{(T)}$, $C^* = C'$ or $C^{(T)}$

Algorithm 2 Reward-Aligned Preference Optimization (RewardDPO)

Input: Instruction I, initial layout L_0, SFT model f_θ, reward function $R(\cdot)$
Output: Trained layout model via Direct Preference Optimization

function SUPERVISEDFINETUNING($\mathcal{D}_{\text{SFT}}$) triplet $(L_0, I, L_{\text{target}}) \in \mathcal{D}_{\text{SFT}}$
    Train model f_θ with $\mathcal{L}_{\text{SFT}} = -\log P_\theta(L_{\text{target}} \mid I, L_0)$

end function

function GENERATEPREFERENCEPAIRS($f_\theta, R(\cdot), \delta$) (L_0, I)
    Generate candidate layouts $\{\tilde{L}_j\}$ using f_θ or constrained decoding
    $L^+ \leftarrow \arg\max_{\tilde{L}_j} R(\tilde{L}_j)$
    if L^+ violates constraints **then continue**
    end if
    Sample transformation $T_k \in \mathcal{T}$ and apply $L^- = T_k(L^+)$
    if $R(L^+) - R(L^-) \geq \delta$ and L^- violates constraints **then**
        Add (I, L_0, L^+, L^-) to $\mathcal{D}_{\text{pref}}$
    end if

    return $\mathcal{D}_{\text{pref}}$
end function

function DIRECTPREFERENCEOPTIMIZATION($\mathcal{D}_{\text{pref}}, \beta$) $(I, L_0, L^+, L^-) \in \mathcal{D}_{\text{pref}}$
    Compute:

$$\mathcal{L}_{\text{DPO}}(\theta) = -\log \frac{e^{\beta \log P_\theta(L^+ | I, L_0)}}{e^{\beta \log P_\theta(L^+ | I, L_0)} + e^{\beta \log P_\theta(L^- | I, L_0)}}$$

    Update f_θ to minimize $\mathcal{L}_{\text{DPO}}$

end function

Step 1: SUPERVISEDFINETUNING($\mathcal{D}_{\text{SFT}}$)
Step 2: $\mathcal{D}_{\text{pref}} \leftarrow$ GENERATEPREFERENCEPAIRS($f_\theta, R(\cdot), \delta$)
Step 3: DIRECTPREFERENCEOPTIMIZATION($\mathcal{D}_{\text{pref}}, \beta$)

Reward Configuration	Posters (SC / LS)	Websites (SC / LS)	Images (SM / DL / Overlap)
All Rewards (Full)	**4.25 / 4.38**	**4.18 / 4.30**	**4.35 / 4.20 / 4.25**
w/o Alignment	4.10 / 4.22	4.05 / 4.16	4.30 / 4.18 / 4.20
w/o Semantic Order	4.05 / 4.18	3.98 / 4.10	4.32 / 4.20 / 4.25
w/o Cross-Sect. Consistency	4.08 / 4.15	4.00 / 4.12	– / – / –
w/o Overlap	4.22 / 4.28	4.15 / 4.25	4.10 / 4.15 / 3.90
w/o Whitespace	4.18 / 4.24	4.12 / 4.20	– / – / –
Only Semantic (SemOrder + XSec)	4.00 / 4.10	3.95 / 4.05	4.32 / – / –
Only Spatial (Align + Overlap)	4.20 / 4.35	4.14 / 4.28	**4.35 / 4.20 / 4.25**

Table 16: Ablation of reward components used in RefineLoop, evaluated via GPT-4o against gold references. Semantic Consistency (SC), Layout Similarity (LS), Semantic Match (SM), Depth Layering (DL), and Overlap realism are scored 1–5. Removing alignment or semantic ordering leads to the largest drops in structured domains; overlap feedback is most critical in image edits.

Model	Avg. SC (1–5) ↑	Avg. LS (1–5) ↑
LayoutPrompter (Lin et al., 2023)	-	4.00 (±0.00)
LLaMA (ZS)	4.08	3.88 (-0.12)
LLaMA + Reward-Refine	4.05	4.10 (+0.10)
LLaMA + RewardDPO	4.18	4.22 (+0.22)
Gemma (ZS)	4.02	3.75 (-0.25)
Gemma + Reward-Refine	3.90	4.05 (+0.05)
LLaMA + RewardDPO	4.08	4.22 (+0.22)
LLaVA (ZS)	3.95	3.60 (-0.40)
LLaVA + Reward-Refine	3.85	3.80 (-0.20)
Gemini-Pro (ZS)	4.38	4.20 (+0.20)
Gemini-Pro + Reward-Refine	4.32	4.36 (+0.36)
GPT-4o (ZS)	4.45	4.30 (+0.30)
GPT-4o + Reward-Refine	**4.50**	**4.45 (+0.45)**

Table 17: Reference-based evaluation on **SMARTEditBench-Websites**, comparing Zero-Shot, Reward-Refine, and RewardDPO-enhanced variants. We report average scores (1–5) for *Semantic Consistency (SC)* and *Layout Similarity (LS)*, with deltas from the **LayoutPrompter** baseline (LS = 4.00) shown in parentheses.

Algorithm 3 Object Translation and Insertion

```
function TranslateObject(layout, section_id, dx, dy)
    [x1, y1, x2, y2] ← layout[section_id].bbox
    layout[section_id].bbox ← [x1 + dx, y1 + dy, x2 + dx, y2 + dy]
    return layout
end function
function ShiftObjectsAfter(layout, anchor_id, dy)
    anchor_y ← layout[anchor_id].bbox[1]
    for all (object_id, object) in layout do
        if object.bbox[1] ≥ anchor_y then
            layout ← TranslateObject(layout, object_id, 0, dy)
        end if
    end for
    return layout
end function
function InsertObject(layout, object_id, bbox, text)
    layout[object_id] ← {bbox : bbox, text : text}
    return layout
end function
```

Algorithm 4 Text Update, Bounding Box, and Reordering

```
function UpdateObjectText(layout, object_id, new_text)
    layout[object_id].text ← new_text
    return layout
end function
function ReplaceObjectBox(layout, object_id, new_bbox)
    layout[object_id].bbox ← new_bbox
    return layout
end function
function ReorderObjects(layout, order, x_start, width, y_padding)
    y ← 100
    for all object_id in order do
        height ← layout[object_id].bbox[3] − layout[object_id].bbox[1]
        layout[object_id].bbox ← [x_start, y, x_start + width, y + height]
        y ← y + height + y_padding
    end for
    return layout
end function
```

Model	Setting	Edit-Ad ↑	Semantic Consistency		Visual-Spatial Layout		
			Narrative ↑	Cross-Sect. ↑	Overlap ↓	Whitespace ↓	Alignment ↑
GPT-4o	Zero-Shot (ZS)	4.45	0.40	**0.59**	-78.0	-4.2	30.0
	Few-Shot (FS)	4.53	0.41	**0.61**	-75.0	-4.1	30.5
	CoT	4.58	0.43	**0.64**	-72.0	-3.9	31.0
	SE (Reward-Refine)	**4.60**	0.44	**0.66**	-70.0	-3.8	31.5
Gemini-Pro	Zero-Shot (ZS)	4.38	0.38	**0.57**	-80.0	-4.5	29.5
	Few-Shot (FS)	4.47	0.39	**0.59**	-78.0	-4.3	30.0
	CoT	4.52	0.41	**0.61**	-75.0	-4.1	30.5
	SE (Reward-Refine)	4.56	0.42	**0.63**	-72.0	-4.0	31.0
Gemma	Zero-Shot (ZS)	4.02	0.28	0.42	-85.0	-5.5	28.0
	Few-Shot (FS)	4.18	0.30	0.44	-82.0	-5.3	28.5
	COT	4.24	0.31	0.45	-80.0	-5.0	29.2
	SE (Reward-Refine)	4.27	0.32	0.47	-78.0	-4.8	30.0
LLaVA	Zero-Shot (ZS)	3.95	0.25	0.39	-155.0	**-7.5**	27.0
	Few-Shot (FS)	4.00	0.26	0.40	-150.0	**-7.2**	27.5
	CoT	4.08	0.28	0.41	-145.0	**-6.9**	28.0
	SE (Reward-Refine)	4.12	0.29	0.43	-140.0	**-6.6**	29.0
LLaMA	Zero-Shot (ZS)	4.08	0.29	0.44	-78.0	-5.5	30.0
	Few-Shot (FS)	4.16	0.30	0.45	-75.0	-5.2	30.5
	CoT	4.22	0.32	0.46	-72.0	-5.0	31.0
	SE (Reward-Refine)	4.28	0.33	0.47	-70.0	-4.8	31.5
Qwen	Zero-Shot (ZS)	4.20	0.27	0.43	-82.0	-5.0	29.5
	Few-Shot (FS)	4.34	0.28	0.44	-80.0	-4.8	30.2
	CoT	4.40	0.30	0.45	-78.0	-4.6	30.8
	SE (Reward-Refine)	4.47	0.31	0.46	-75.0	-4.5	31.0

Table 18: Reference-Free Evaluation of Models on **SMARTEditBench-Websites**. Compared to posters, models struggle even more with visual-spatial layout editing on websites—showing higher overlap and whitespace penalties and lower alignment consistency.

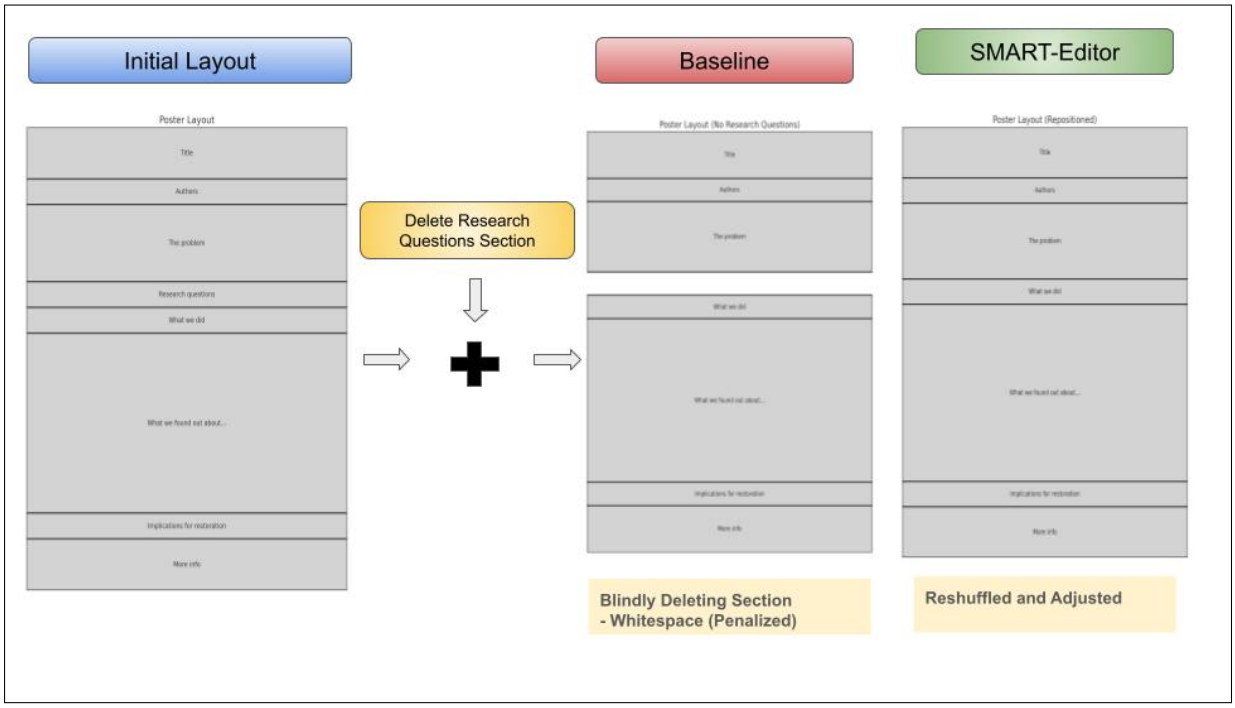

Figure 7: Reward improvement over iterations across semantic and visual dimensions on the posters, websites and natural images. Semantic consistency shows minimal gains across iterations for natural images, while visual-spatial layout rewards improve more sharply for posters and websites.

Algorithm 5 object Removal, Resizing, and Alignment

function REMOVEOBJECT($layout, object_id$)
  delete $layout[object_id]$
  return $layout$
end function
function RESIZEOBJECT($layout, object_id, scale_x, scale_y$)
  $[x_1, y_1, x_2, y_2] \leftarrow layout[object_id].bbox$
  $cx \leftarrow (x_1 + x_2)/2, cy \leftarrow (y_1 + y_2)/2$
  $width \leftarrow (x_2 - x_1) \cdot scale_x$
  $height \leftarrow (y_2 - y_1) \cdot scale_y$
  $layout[object_id].bbox \leftarrow [cx - width/2, cy - height/2, cx + width/2, cy + height/2]$
  return $layout$
end function
function ALIGNOBJECTLEFT($layout, object_id, x_ref$)
  $[x_1, y_1, x_2, y_2] \leftarrow layout[object_id].bbox$
  $width \leftarrow x_2 - x_1$
  $layout[object_id].bbox \leftarrow [x_ref, y_1, x_ref + width, y_2]$
  return $layout$
end function

Algorithm 6 Centering and Snapping to Grid

function CENTEROBJECT($layout, object_id, canvas_width$)
  $[x_1, y_1, x_2, y_2] \leftarrow layout[object_id].bbox$
  $width \leftarrow x_2 - x_1$
  $cx \leftarrow canvas_width/2$
  $layout[object_id].bbox \leftarrow [cx - width/2, y_1, cx + width/2, y_2]$
  return $layout$
end function
function SNAPTOGRID($layout, object_id, grid_unit$)
  $bbox \leftarrow layout[object_id].bbox$
  $snapped \leftarrow$ round each coordinate in $bbox$ to nearest multiple of $grid_unit$
  $layout[object_id].bbox \leftarrow snapped$
  return $layout$
end function

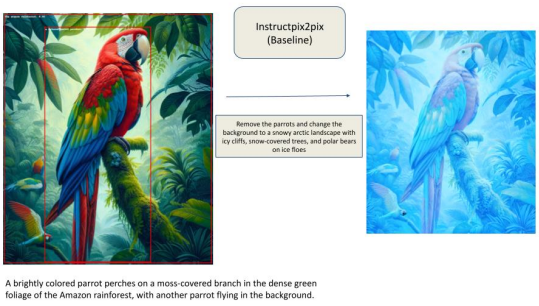

Figure 8: Natural-Image (InstructPix2Pix).

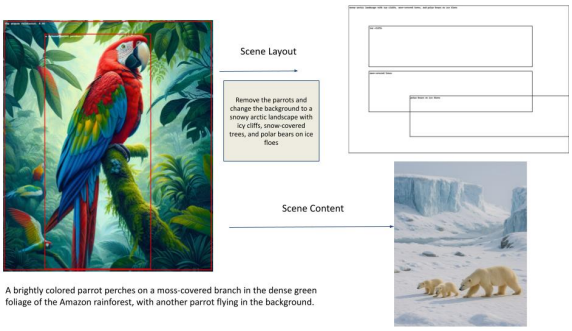

Figure 9: Natural-Image (SMART-Editor)

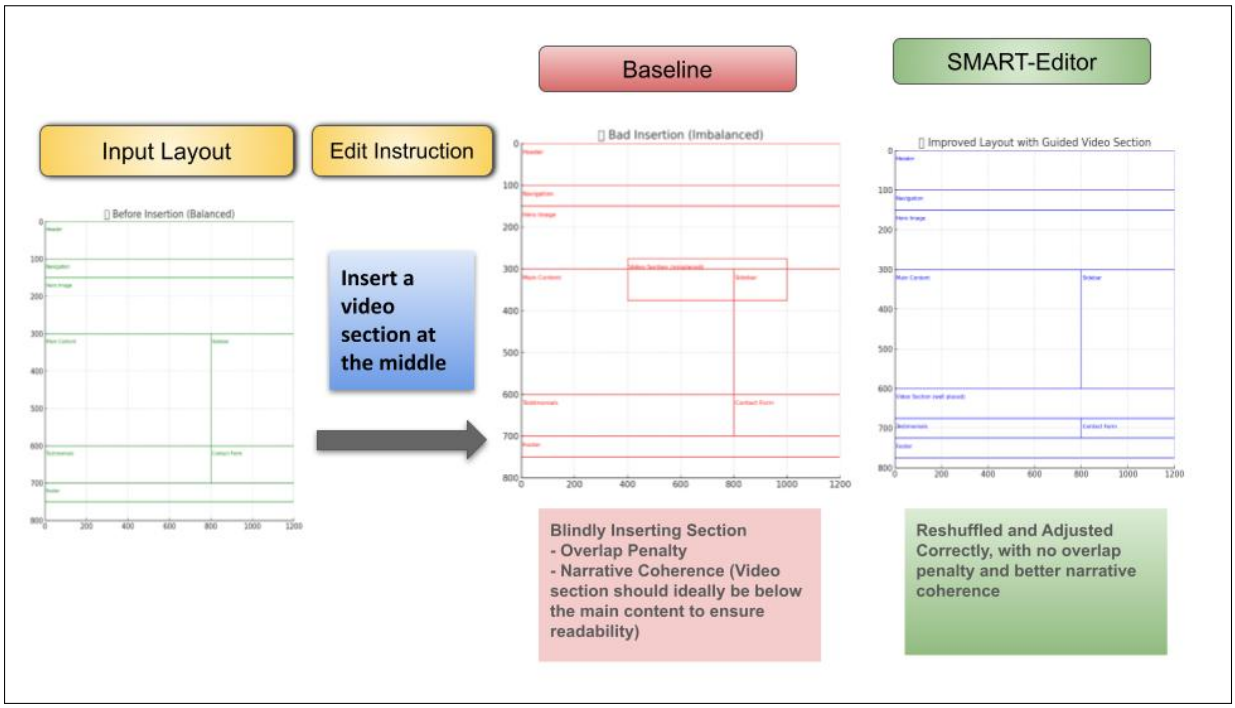

Figure 10: Reward improvement over iterations across semantic and visual dimensions on the posters, websites and natural images. Semantic consistency shows minimal gains across iterations for natural images, while visual-spatial layout rewards improve more sharply for posters and websites.

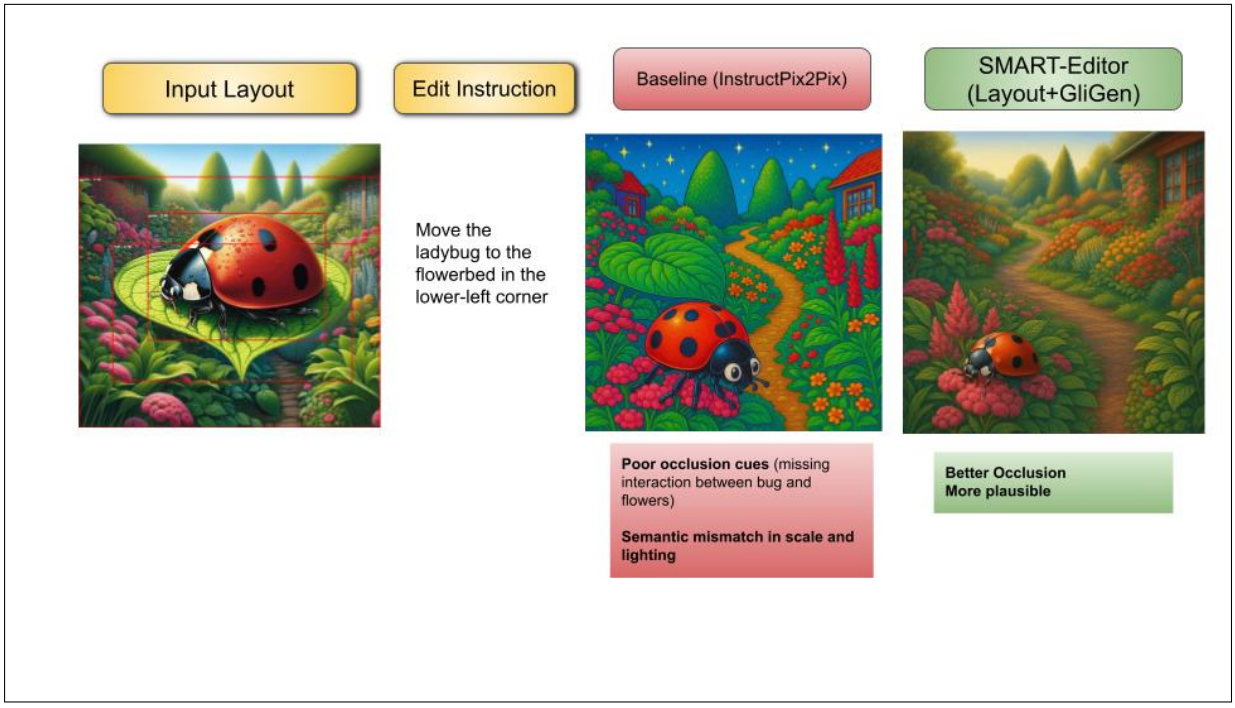

Figure 11: Reward improvement over iterations across semantic and visual dimensions on the posters, websites and natural images. Semantic consistency shows minimal gains across iterations for natural images, while visual-spatial layout rewards improve more sharply for posters and websites.

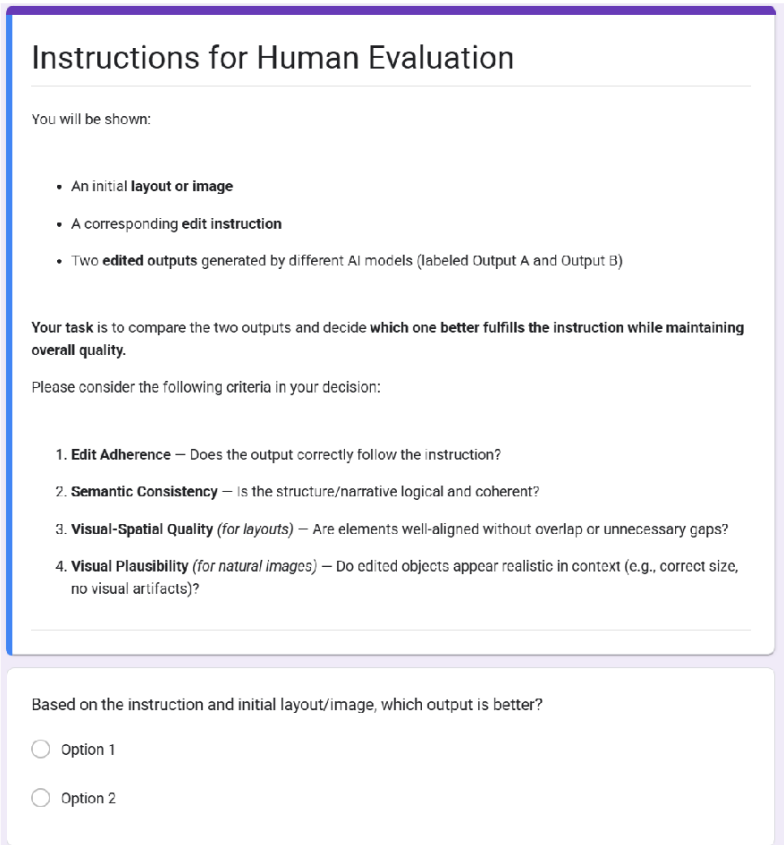

Instructions for Human Evaluation

You will be shown:

- An initial **layout or image**
- A corresponding **edit instruction**
- Two **edited outputs** generated by different AI models (labeled Output A and Output B)

Your task is to compare the two outputs and decide **which one better fulfills the instruction while maintaining overall quality.**

Please consider the following criteria in your decision:

1. **Edit Adherence** — Does the output correctly follow the instruction?
2. **Semantic Consistency** — Is the structure/narrative logical and coherent?
3. **Visual-Spatial Quality** *(for layouts)* — Are elements well-aligned without overlap or unnecessary gaps?
4. **Visual Plausibility** *(for natural images)* — Do edited objects appear realistic in context (e.g., correct size, no visual artifacts)?

Based on the instruction and initial layout/image, which output is better?

- ◯ Option 1
- ◯ Option 2

Figure 12: Human Evaluation Instructions

You are invited to participate in a research study conducted as part of an academic project to evaluate the quality of AI-generated edits to layouts and images. This study involves viewing edit instructions, initial layouts or images, and evaluating outputs generated by different models.

Purpose of the Study:
To assess whether AI models can make semantically and visually coherent edits that align with human design intuition.

What You Will Do:
You will be shown:

- An initial layout or image
- An edit instruction
- Two edited outputs (Output A and Output B)

You will compare these outputs and indicate which one is better based on how well the instruction is followed and the overall layout/image quality.

Estimated Time:
This task will take approximately **10–15 minutes** in total.

Voluntary Participation:
Your participation is completely voluntary. You may skip any question or stop the survey at any time.

Confidentiality:
No personally identifiable information will be collected. Your responses will be used for research purposes only.

Compensation:
You will be compensated according to the agreement with the research team or platform (e.g., Upwork, university lab, etc.).

Contact Information:
If you have questions about the study, please contact the research team at [YOUR EMAIL].

Figure 13: Consent Form from participants